Laser & Photonics Reviews

LASER & PHOTONICS REVIEWS

www.lpr-journal.org

REVIEW OPEN ACCESS

Mechanical Properties and Testing Strategies for Two-Photon Lithography: A Review of Current Practices and Emerging Challenges

Dalila Fontana[1] | Edoardo Rossi[2] | Marco Sebastiani[2] | Edoardo Bemporad[2,3] | Angelo Accardo[4] | Alberto Rainer[1,5] | Enrico D. Lemma[1,5]

[1]Department of Engineering, Università Campus Bio-Medico Di Roma, Rome, Italy | [2]Università degli Studi Roma Tre, Department of Civil, Computer Science and Aeronautical Technologies Engineering, Rome, Italy | [3]Institute For Polymers, Composites and Biomaterials - National Research Council, Pozzuoli, Naples, Italy | [4]Department of Precision and Microsystems Engineering, Faculty of Mechanical Engineering, Delft University of Technology, Delft, The Netherlands | [5]Institute of Nanotechnology (NANOTEC), National Research Council, Lecce, Italy

Correspondence: Enrico D. Lemma (e.lemma@unicampus.it)

Received: 24 December 2025 | **Revised:** 18 June 2026 | **Accepted:** 20 June 2026

Keywords: 3d printing | characterization methods | lithography | materials science | metamaterial | micro tensile | nanoindentation | nanotechnology | photoresist | two-photon physics

ABSTRACT

Two-photon lithography (2PL) is a high-resolution additive manufacturing technique achieving complex three-dimensional (3D) microstructures with sub-micrometer precision. This capability has driven applications across optics, microfluidics, bioelectronics, metamaterials, and biomedical engineering. Beyond geometry, the functionality of 2PL-fabricated structures critically depends on their mechanical properties, which are influenced by resin chemistry, printing parameters, and post-processing treatments. Understanding the mechanical behavior of 2PL-fabricated structures at both macro- and micro-scales is essential for the rational design and development of advanced devices and systems. Accordingly, this review provides the reader with a concise yet comprehensive overview of the current knowledge on the mechanical properties of materials usually employed in 2PL. Common photoresist classes (e.g., hydrogel-like, elastomeric polymer networks, rigid glassy polymers, and hybrid organic–inorganic networks) offer distinct trade-offs in stiffness, with Young's modulus spanning several orders of magnitude. Mechanical performance can be further tuned via laser settings, environmental conditions, or post-processing approaches such as UV curing, pyrolysis, or incorporation of responsive chemistries for dynamic "4D" behavior. We then examine the methodologies applied—or specifically developed—to characterize 2PL materials and microstructures in terms of stiffness, toughness, and viscoelastic response at the micro- and nanoscale. Finally, we discuss the applications where mechanical properties are critical to the functionality of 2PL structures, such as tissue engineering, microfluidics, and tunable metamaterials. Looking ahead, advances in material design, adaptive characterization, and predictive modeling will enable rational, data-driven workflows. Treating mechanical properties as fundamental design parameters will be key for developing reliable microdevices for next-generation technologies.

1 | Introduction

Two-photon lithography (2PL), also referred to as two-photon polymerization or direct laser writing, is an advanced additive manufacturing technique enabling the fabrication of complex 3D microstructures with sub-micrometer resolution. This method leverages a nonlinear process in which the simultaneous absorption of two photons initiates localized polymerization exclusively at the focal point of a pulsed laser beam. As a result, 2PL achieves high spatial resolution while minimizing off-target exposure. Owing to this capability, 2PL has become an attractive method for fabricating miniaturized optical, mechanical, and multifunctional devices, with applications spanning optics [1, 2], microfluidics [3, 4], bioelectronics [5, 6], metamaterials [7, 8], and biomedical research [9–11]. A critical aspect of the design and application of 2PL-fabricated structures lies in understanding and controlling their mechanical properties. Indeed, the functional behavior of a 3D structure depends not only on its geometry, but also on its intrinsic material characteristics and on their interaction with experimental conditions. For instance, in the case of scaffolds for cell biology studies, often the 3D structure not only hosts the cells undergoing investigation, but constitutes itself an experimental variable, being able to significantly influence cell behavior, e.g., by providing a soft/stiff substrate, thus inducing specific phenotypic and genotypic responses well known in 2D systems [12].

This review is grounded in the recognition that the mechanical properties of photoresists play a key role in determining the behavior of 2PL microstructures, alongside other fundamental features, such as chemical composition and functional responsiveness. Understanding the mechanical behavior of 2PL-fabricated structures at both macro- and micro-scales is essential for the rational design and development of advanced devices and systems. Accordingly, this review aims to provide a concise yet comprehensive overview of current knowledge regarding the mechanical properties of materials commonly used in 2PL, with particular emphasis on Young's modulus. We then examine the methodologies developed or adapted to characterize these properties, offering insight into the state of the art in mechanical characterization techniques for 2PL materials and microstructures. Recognizing that measuring material properties is often a means to enable functionality rather than an end in itself, we conclude by presenting representative examples of 2PL-fabricated architectures that leverage specific mechanical properties to address fundamental research challenges.

In summary, this manuscript is intended as a practical reference for researchers newly approaching 2PL, guiding them in identifying the most relevant mechanical properties and characterization methods for 2PL materials. At the same time, it aims to serve experienced scientists by providing them with a logically structured compilation of references, facilitating efficient access to functional information, and supporting the design of experiments.

2 | Materials for 2PL and Mechanical Properties

Over the years, a plethora of photoresists have been developed for 2PL, and several reviews available in the literature provide detailed insights into the most commonly used materials [1, 13–19]. While commercial resins are still the most employed, many research groups have formulated custom materials to achieve specific mechanical and chemical properties, tailored to intended applications.

In general, 2PL relies on the radical or cationic polymerization of monomeric units. The former is based on the production of light-induced radical species by the initiator, followed by propagation of the polymerization: when the individual monomers (e.g., acrylates) add sequentially to a single active chain end, the process is referred to as chain-growth, while in step-growth polymerization, reactive groups on different monomers/oligomers react randomly to link together (as in thiol-ene chemistry). Instead, cationic polymerization relies on transferring a cationic charge from growing polymeric chains to nucleophilic monomers or oligomers, e.g., in the case of vinyl- or epoxy-based monomers. At the termination of the process, the percentage of reactive groups that have reacted to form the polymer network is defined as the degree of crosslinking, which is directly related to the resulting mechanical properties of the material. According to their mechanical behavior, materials for 2PL can be broadly subdivided into the following categories:

(i) Soft/Hydrogel-like photoresists, with low elastic modulus (kPa-MPa);
(ii) Elastomeric polymer networks, showing moduli in the range of MPa to GPa;
(iii) Rigid glassy polymers, encompassing stiffer materials, usually with low viscoelastic behavior;
(iv) Hybrid organic–inorganic networks and composite resists, usually showing brittle failure and modulus in the range of several GPa.

Soft/Hydrogel photoresists are water-rich polymer formulations that enable the fabrication of swellable 3D micro/nanostructures via 2PL. This class of materials typically exhibits a Young's modulus spanning from the order of ≈1 kPa to ≈10 MPa, comparable to the stiffness of many biological tissues (e.g., from a few hundred pascals in brain tissue up to ≈1 MPa in cartilage or tendons). Indeed, in the case of hydrogels, the crosslink density influences the swelling capability of the material, and the final mechanical properties are directly affected by the amount of water uptake. Three main subcategories can be distinguished: (i) protein-based hydrogels, characterized by protein networks within an aqueous phase (e.g., gelatin [20–24], and silk fibroin-based [25], with tunable Young's modulus between ≈10 and 50 kPa); (ii) polysaccharide-based hydrogels, (e.g., hyaluronic acid vinyl ester (HAVE)/dithiothreitol (DTT) blend, with reported moduli of 86–106 kPa [26]); (iii) synthetic hydrogels, including PEG [27, 28] and pNIPAM derivatives [29, 30], HEMA, acrylamide and others [31–34].

Elastomeric polymer networks usually rely on radical polymerization of monomers with high average molecular weight containing at least two carbon-carbon double bonds, but in this class, also other chemical (co)-polymerization mechanisms might be included (e.g., step-growth polymerization [35], thiol-ene chemistry [36], reversible addition-fragmentation chain transfer polymerization [37], nitroxide mediated polymerization [37]).

Although the resulting stiffness may be -even significantly- modulated based on network composition and crosslinking density, generally the stiffness of these materials is in the range of several MPa to a few GPa, and shows a clearly evident viscoelastic behavior [38, 39]. A number of commercial acrylate-based formulations are available, including most of the photoresists belonging to the IP series developed by Nanoscribe GmbH [40–46], together with materials produced by UpNano GmbH [47], MicroResist GmbH, and IQS [48]. Numerous research groups have explored custom formulations, with pentaerythritol triacrylate [28], pentaerythritol tetraacrylate, and trimethylolpropane ethoxylate triacrylate among the most widely employed [28, 29]. Photoinitiators, typically incorporated at concentrations between 0.01 and 5 wt%, play a critical role in defining the mechanical properties of the fabricated structures.

Rigid glassy polymers easily reach several GPa stiffness and relatively high tensile strength, and might show a less evident viscoelastic behavior with respect to softer counterparts [47, 49–51]. In this case, radical polymerization is the most common mechanism, leading to high crosslinking density or degree of conversion. This category is mainly populated by short-chained acrylate-based formulations, but original strategies to obtain glassy polymers via 2PL have been proposed [52].

Hybrid organic–inorganic networks and composite resists are obtained by incorporating nanofillers into a polymer matrix or by applying functional coatings. The modification of a basic resist may be aimed at: (i) introducing additional functionalities to the material, or (ii) mechanically reinforcing the material. In the first case, mechanical properties are usually not significantly affected. For example, conductive fillers can be included to introduce a conductive behaviour, retaining at the same time the softness of a hydrogel structure, e.g., in the case of PEDOT:PSS incorporated in methacrylated gelatin [53] or polyethylene oxide [54], or the stiffness of an acrylated formulation [55]. Additionally, other strategies [56] were also explored to confer functionality to resists, including the deposition of conductive layers on structures made via conventional photoresists [5], or the integration/decoration with metal/silica nanoparticles [57–61], carbon nanotubes [56, 62], or graphene [63]. Alternatively, the aim of including nanofillers may also consist of enhancing stiffness. For instance, Ovsianikov et al. introduced zirconium propoxide into a MAPTMS-based sol–gel system to obtain the hybrid SZ2080 [64, 65], where inorganic Zr–O–Si bonds strongly reduce the material shrinkage during polymerization, and significantly improve mechanical stability, as more recently shown by Pertoldi and colleagues [66]. The commercial Ormocomp family, produced by MicroResist Technology GmbH, represents another example of hybrid photoresists, combining silica-based components within an acrylate matrix [49]. To further increase the stiffness of architectures such as nanolattices—which, despite being fabricated from intrinsically rigid resists, exhibit reduced mechanical strength due to their porous geometry—thin metal or oxide coatings can be applied. Fundamental works by Jang et al. [67] and Meza et al. [68] exploited the principle of fabricating lattices via 2PL, which were then covered with TiN and alumina via atomic layer deposition, respectively, and then etched out via plasma cleaning. This left ceramic hollow structures showing exceptionally high mechanical performance yet presenting low density and ordered hierarchy with length scales comparable to those found in several biological materials. In turn, Maggi et al. [69] demonstrated that such coatings increased the Young's modulus from sub-MPa values to approximately 100 MPa, enhancing scaffold suitability for cell growth. Finally, another subclass of hybrid organic-inorganic materials for 2PL may be identified, including preceramic- or silica-containing resists for which stiffness increases only after thermal post-processing by conversion of the inorganic fillers. This usually leads to mechanical and optical properties, and thermal and chemical resistance comparable to commercial fused silica glass [70].

Figure 1 summarizes the main properties of commercially available and custom-made 2PL resins based on current literature.

In summary, each class of photoresists offers distinct trade-offs, making material selection critical for designing 3D microstructures, especially when specific mechanical properties and functionality are required.

2.1 | Techniques for Enhancing Mechanical Properties

Studies have shown that the mechanical properties of microstructures fabricated via 2PL can be tuned by adjusting key printing parameters. In particular, the Young's modulus of commercial and custom acrylate-based photoresists correlates not only with laser power [28, 71, 72], but also with printing speed [73] and geometry discretization parameters, commonly referred to as slicing (along the z-axis) and hatching (along the x- and y-axes) [74, 75]. In some cases, these variations can be substantial, reaching up to an order of magnitude [40]. Recently, a single-component resist demonstrated extreme stiffness variability as a function of exposure dose during polymerization [35]. Furthermore, immersion in water can significantly reduce the Young's modulus of a given material, an important consideration when designing photoresists for biological applications [34, 40].

Beyond printing parameters, post-processing techniques offer additional opportunities for tuning mechanical properties. For example, UV post-curing has been reported to increase the Young's modulus of acrylate resins [76]. Alternatively, the exploitation of chemical (click) reactions may reinforce the material structure: for example, incorporating anthracene moieties into acrylate-based photoresists enables the formation of anthracene dimers upon prolonged exposure to visible light at 415 nm, resulting in increased stiffness and hardness [77]. Similarly, thiol-ene chemistry [36, 78] and nitroxide-mediated polymerization [79] were exploited to achieve structures with improved mechanical properties.

A well-established method for substantially increasing the stiffness of 2PL-fabricated structures is post-exposure carbonization via pyrolysis. Although this treatment typically induces significant shrinkage [80–84], it can yield up to a ten-fold increase in Young's modulus [85], depending on both the polymerization parameters applied prior to pyrolysis and the temperature and duration of the carbonization treatment [86]. Interestingly, recent findings by Zhang et al. challenge the assumption that pyrolyzed structures are inherently brittle. Their study showed that 2PL-fabricated micropillars (approximately 2 μm in diameter) exhib-

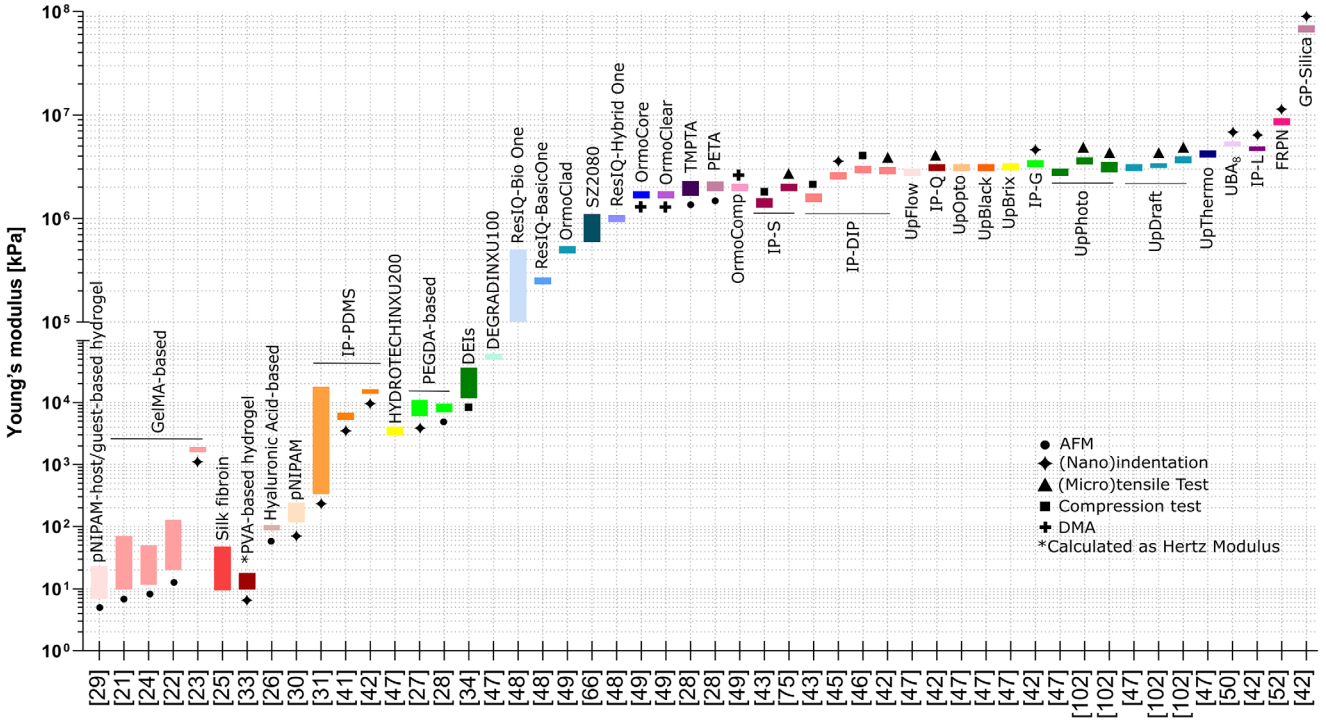

FIGURE 1 | Overview of Young's modulus of widely used materials for 2PL reviewed in this work. Where possible, characterization methods were included. References are indicated in square brackets.

ited rubber-like behavior, sustaining compressive strains of ≈50% without catastrophic failure [87]. This opens new possibilities for designing mechanically robust yet flexible microarchitectures using 2PL.

In recent years, the concept of 4D materials [88] has been extended to the field of 2PL. This refers to 3D microstructures capable of reversible changes in mechanical properties, along with shape deformation or swelling, in response to external physical, chemical, thermal, or optical stimuli. Such dynamic behavior offers a powerful route for imparting novel functionalities to conventional 2PL materials and geometries. The development and application of stimuli-responsive 4D materials, as well as the evolving understanding of their dynamic behavior, have been extensively reviewed, as these have contributed to the design and realization of adaptive and multifunctional microstructures in fields such as soft robotics, biomedical devices, and smart sensors [10, 13, 29, 30, 89–99].

3 | Characterization Techniques

When characterizing the mechanical properties of materials at the microscale, selecting the right methodology is crucial. Experimental procedures at this scale typically require greater precision and effort compared to standard macroscale tests. For example, performing tensile tests on dog-bone-shaped specimens only a few micrometers wide—intended to measure parameters such as Young's modulus, elongation at break, and maximum strength—poses significant challenges. These difficulties stem from the complexity and sensitivity of the required equipment, including micromanipulators operated within scanning electron microscopes [45]. Consequently, widely adopted standards for materials testing, such as ISO 527-2 for tensile properties and ISO 48-4 for hardness [100, 101], may not be easily applied to 2PL-fabricated microstructures, which induced researchers to develop standardizable characterization strategies tailored to the unique scale and fabrication constraints of 2PL [102]. On the other hand, approaches and technologies to characterize mechanical properties directly at the microscale may present advantages that macroscopic tests do not provide, including nanometric precision in the evaluation of the measured properties.

3.1 | Nanoindentation and Atomic Force Microscopy (AFM)

As already stated, the dose delivered by the pulsed laser beam in a 2PL system defines the voxel dimensions, and in turn the crosslinking density of the resulting polymerized material. In principle, the dose—which correlates to the laser power—may be significantly tuned within the same structure. As a consequence, the resulting mechanical response can also considerably differ within a single microstructure. Conventional bulk tests are blind to these gradients, whereas nanomechanical techniques, most notably instrumented nanoindentation and atomic force microscopy (AFM), provide the spatial resolution to detect them.

3.1.1 | Nanoindentation of Two-Photon-Polymerized Materials

Among the panoply of micromechanical techniques available for small-scale materials, instrumented nanoindentation remains the most versatile and quantitatively robust method for probing local mechanical behavior (Figure 2A). Its principle is con-

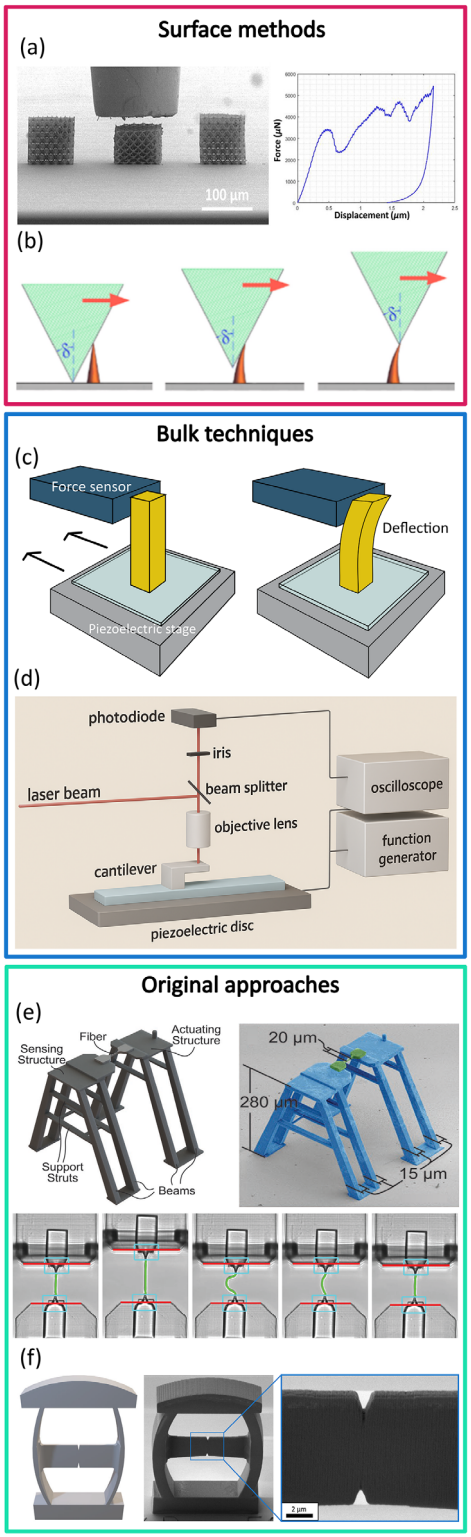

FIGURE 2 | Selection of methodologies for mechanical characterization of 2PL materials. The classification refers to the main categories identified in this work: surface methods, which include nanoindentation (panel (a), adapted with permission [111] Copyright 2020, Elsevier), and atomic force microscopy (panel (b), adapted with permission [115] Copyright 2021, Elsevier); bulk techniques, which do not rely on models to infer mechanical properties from surface measurements (panels (c) and (d), adapted with permission [71] Copyright 2017, IEEE, and [66], Copyright 2020, AIP Publishing, respectively); original approaches to mechanical characterization of materials and 3D structures microfabricated via 2PL (panels (e) and (f), adapted with permission [130] Copyright 2023, Elsevier, and [44] Copyright 2023, Wiley, respectively).

ceptually simple: a hard tip of known geometry (commonly a three-sided Berkovich pyramid [103] or a spherical/conospherical diamond) is pressed into the surface of a material while recording the applied load (P) and the resulting penetration depth (h). The resulting P–h curve embodies the material resistance to elastic and plastic deformation. The widely adopted Oliver–Pharr model enables the evaluation of nanoindentation measurements, starting from the definition of contact stiffness (S) during unloading:

$$S = \left.\frac{dP}{dh}\right|_{h_{max}}$$

which defines the reduced modulus E_r:

$$E_r = \frac{S}{2\sqrt{\pi A_c}}$$

where A_c is the projected contact area. The intrinsic elastic modulus E of the specimen is obtained from:

$$\frac{1}{E_r} = \frac{1-\nu^2}{E} + \frac{1-\nu_i^2}{E_i}$$

with E_i , ν_i the indenter constants.

To extend the static indentation framework and allow the measurement of depth-dependent properties of materials in a single step, modern nanoindenters implement Continuous Stiffness Measurement (CSM), in which a small oscillatory load is superimposed on the quasi-static loading signal. This dynamic load on top of the static load is then used to measure the stiffness, which is further processed to calculate the modulus and hardness of the material. Indeed, this dynamic excitation—typically a sinusoidal force at frequencies between 1 and 200 Hz—enables real-time determination of contact stiffness and phase lag as a function of penetration depth. From these data, one obtains the storage modulus E', representing the recoverable elastic response, and the loss modulus E'', quantifying energy dissipation due to viscoelasticity. The ratio $\tan\delta = E''/E'$ serves as a reliable indicator of time- or frequency-dependent deformation, revealing transitions from glassy to rubber-like behavior in soft or partially cross-linked 2PL materials. Since stiffness and phase information are continuously acquired during loading, CSM enables depth-resolved profiling of modulus gradients, detection of interfacial layers, and assessment of curing heterogeneity within printed voxels—features particularly relevant to 2PL materials, where polymerization kinetics and network density vary over sub-micrometer scales.

In 2PL architectures, even under constant laser power and writing speed, individual voxel volumes may exhibit varying degrees of conversion due to local factors affecting polymerization. This does not necessarily imply that the overall mechanical properties of 2PL structures are inhomogeneous; rather, nanoindentation provides a means to bridge processing physics and mechanical functionality down to the mechanical signature of a single written layer [102].

The robustness of this method is well documented. Belqat et al. [28] demonstrated that by probing PEGDA-, TMPTA-, and PETA-based resins, indentation spans three orders of magnitude solely through variations in laser power and scan strategy. The implication is clear: indentation becomes a tool to infer crosslink density as a function of printing parameters.

The versatility of the technique is further highlighted by Eivgi et al. [104], who validated nanoindentation for soft, adhesive elastomers—where conventional approaches often fail. Their protocol, built around a small-radius conospherical tip and a trapezoidal displacement path with dwell and lift-off control, captured the viscoelastic drag and adhesion that would otherwise distort an Oliver–Pharr analysis. Adoption of a nano-JKR [105] contact model revealed how adhesion can inflate apparent moduli by up to 80%, a critical correction for compliant 2PL materials to be used in soft robotics and biointerfaces.

Even for soft networks (3–4 MPa), nanoindentation remains precise enough to resolve microstructural transitions. The same logic extends to coupled spectroscopic approaches: Schweiger et al. [106] correlated Raman-derived conversion ratios (C═C/C═O band ratio) with indentation moduli in IP-Dip and IP-Q structures, demonstrating a direct, quantitative link between polymerization degree and mechanical stiffness.

Collectively, these studies converge on a coherent picture: nanoindentation elucidates the interplay between 2PL process parameters and the resulting spatial distribution of stiffness. It functions as a mapping probe of crosslinking, with load-displacement data replacing absorbance spectra (e.g., in the case of dry polymers) or complementing micro-Raman or -FTIR spectroscopy (e.g., in the case of swollen hydrogels) as a fingerprint of the voxel polymerization state.

3.1.2 | Compression Testing Using the Nanoindenter as a Force Actuator

While Oliver–Pharr indentation extracts moduli from unloading stiffness, the same instrument can be repurposed as a micro-compression platform by using a flat-punch tip to impose uniaxial strain on micro- or nano-pillars, unit cells, or complex metamaterials—architected materials that behave as homogeneous media when their periodicity is much smaller than the characteristic structural dimension. In this configuration, the nanoindenter acts not as a hardness tester but as a precision load-displacement actuator and sensor [107, 108]. No contact-area model or unloading analysis is required; instead, the compressive response of the printed material is directly recorded, and the stress–strain curve is obtained by computing the appropriate cross-sectional area.

This approach developed alongside the rise of mechanical metamaterials as a distinct class of materials whose geometry governs mechanical performance (Section 5.2). Early experimental and theoretical work by Bauer and Valdevit [109, 110] demonstrated how micro- and nanolattices fabricated via 2PL exhibit stiffness-density scaling laws comparable to those observed in metallic and ceramic lattices. These studies underscored the importance of unit-cell-level testing and inspired the adaptation of nanoindenters into miniature uniaxial testing platforms by equipping actuators with flat punch diamond tips as miniaturized compression plates.

Numerous investigations have since adopted this approach. Examples include studies of buckling and densification modes mimicking those of metallic microlattices (i.e., localized hardening effects akin to strain-gradient plasticity) as reported by Vangelatos et al. [111]: the authors analyzed mechanical isotropy and auxeticity in topologically optimized metamaterials, achieved by coupling finite element predictions of topologies with mechanistic understanding of the different regimes where property homogenization eventually fails.

A major milestone has been the integration of flat-punch nanoindentation with environmental control, enabling measurements in hydrated and reactive media.

Rohbeck et al. [45] advanced this concept by coupling flat-punch micro-compression with variable strain rate and temperature control, testing IP-Dip pillars up to 600 s^{-1} and 80°C. Their work revealed strong rate hardening and thermal softening, modeled through strain rate–temperature superposition, establishing nanoindentation as a dynamic micromechanical platform for viscoelastic 2PL polymers. Methodologically, the flat-punch configuration differs from standard indentation in that no contact-area function is required; however, alignment accuracy is critical, as even slight tilt can induce asymmetric deformation and shear. Contact is established through a pre-load protocol at forces below $1 - 5\ \mu N$, after which the instrument stiffness ensures linear force control. CSM can be incorporated to monitor compliance changes throughout loading. For soft or viscoelastic 2PL materials, frequency (storage and loss modulus) and rate-dependent behavior become central: by varying displacement rate from nanometers to micrometers per second, researchers have mapped apparent yield stress and plateau modulus as a function of strain rate, constructing time–temperature superpositions at the microscale. Such behavior has also been observed in nanoindentation creep and relaxation studies of hydrogel-based 2PL structures [112], confirming that even within a single polymer network, viscoelastic timescales can differ markedly with exposure dose and cross-linking density.

Beyond individual pillars, automated arrays of flat-punch tests now enable a statistical assessment of reproducibility and failure variability [113]. The apparent modulus and strength of 2PL-fabricated structures often follow log-normal distributions, a signature of photon-statistical fluctuations during crosslinking. This statistical dimension highlights an essential aspect of 2PL mechanics: even under nominally identical conditions, stochastic energy absorption and polymerization kinetics introduce local heterogeneities—subtleties that nanoindentation is uniquely sensitive to detect.

3.1.3 | AFM-Based Mechanical Characterization of 2PL Structures

If nanoindentation can be regarded as the quantitative backbone of small-scale mechanical testing, atomic force microscopy

(AFM) represents its complementary, high-resolution counterpart (Figure 2B). Both techniques, when AFM is used in indentation mode, rely on controlled penetration of a sharp probe into the surface, yet their underlying principles differ profoundly. Nanoindentation measures force through the deflection of a rigid load frame with a known geometry, whereas AFM measures deflection directly at the cantilever tip by optical lever detection, converting nanometric bending into a calibrated force. The result is exquisite force sensitivity—often in the nanonewton range—and a spatial resolution defined not by the indentation area, but by the tip radius, which can be as small as 5–10 nm.

The operating principle of the AFM is based on a sharp tip pointing toward the sample in a direction which is perpendicular to the cantilever. This senses the interaction forces generated between the tip and the sample surface, i.e., van der Waals, and electronic repulsions arising at (sub-)nanometric distances. The cantilever and the tip scan the sample via a piezoelectric stage. The deflection of the cantilever in the z direction is measured using a laser beam that is projected on the upper surface of the cantilever, close to the tip. The reflected beam is led to a four-segment photo-diode, usually by means of mirrors. The vertical and lateral deflection, vibration phase, and amplitude of the AFM probe while interacting with the sample are used to investigate surface topography, friction, and elastic properties of the sample. To obtain quantitative results, the relationship describing the interactions between tip and sample surface needs to be established, which is usually done via analytical and numerical models [114].

Practically, AFM enables quantitative nanomechanical measurements in regions inaccessible to conventional nanoindenters, i.e., on delicate membranes, steep topographies, or hydrated environments, where large loading frames would introduce artifacts. Moreover, AFM can simultaneously image and measure, mapping elastic modulus, adhesion, and dissipation across an area while maintaining nanometric lateral resolution. Its limitations mirror its strengths: the achievable load range is low (tens to hundreds of nanonewtons), restricting indentation depth to the near-surface region, and the determination of absolute moduli depends strongly on the chosen contact model (e.g., Hertz, DMT, JKR). Nevertheless, these constraints make AFM ideally suited for probing surface-level and sub-micrometer mechanics of 2PL micro-architectures, where gradients in crosslink density, residual stress, or hydration are often confined to the outer few hundred nanometers of each voxel.

The most direct implementation—force–distance spectroscopy (FDC)—records cantilever deflection during approach and retraction, generating a curve from which elastic modulus, adhesion, and viscoelasticity can be extracted. In the simplest Hertzian approximation for a paraboloidal tip of radius R_{tip}, the contact force F and indentation δ obey:

$$F = \frac{4}{3} E^* \cdot R_{tip}^{\frac{1}{2}} \cdot \delta^{\frac{3}{2}}$$

where E^* is the reduced modulus, analogous to the nanoindentation parameter E_r. From a series of such measurements, AFM can generate modulus maps with nanometric resolution, effectively transforming it from an imaging device into a true mechanical microscope.

In the context of 2PL, this ability to combine topography and mechanics in a single measurement is invaluable. Structures produced by 2PL often exhibit complex 3D morphologies—pillars, bridges, lattices, and membranes—with stiffness variations spanning orders of magnitude over micrometer scales. AFM enables the direct visualization of these heterogeneities. Angeloni et al. [115] leveraged this capability to characterize arrays of nanopillars fabricated by 2PL using the commercial IP-L780 resist. Through contact-mode imaging (CMI) and force-spectroscopy imaging (FSI), they determined the stiffness, adhesion, and failure stress of individual pillars, reporting stiffness values of 13–16 N m^{-1} and failure stress levels around 0.3 GPa, without requiring electron microscopy or conductive coatings. This represents a clear advantage over in situ SEM-based tests that often demand metal coating or vacuum conditions, together with the consideration that AFM usually enables the preservation of the fabricated geometries, given that other destructive events (e.g., structure detachment due to poor adhesion) do not intervene.

Beyond simple force curves, dynamic AFM techniques such as Quantitative Nanomechanical Mapping (QNM) and Intermodulation AFM (ImAFM) enable faster, high-resolution assessment of local viscoelasticity. QNM uses intermittent contact to measure force, deformation, and phase lag at every pixel during raster scanning, achieving kilohertz sampling of local moduli [116–118]. ImAFM advances this further by driving the cantilever at multiple frequencies simultaneously, extracting storage and loss moduli with sub-100 nm lateral resolution [119–121].

Silbernagl et al. [122] applied these methods to dual-cured epoxy–acrylate interpenetrating polymer networks (IPNs) produced by multiphoton lithography. By correlating AFM-derived stiffness maps with laser power and scan velocity, they revealed how radical and cationic curing kinetics create nanoscale domains of differing elasticity.

Another key frontier for AFM is operation in liquid environments, which is crucial for biocompatible or hydrogel-based 2PL systems. Because cantilever deflection is measured optically, AFM remains fully functional in water, thus enabling direct probing of hydrated surfaces at physiologically relevant temperatures. Examples include the work of Dudziak et al. [123], who investigated long-term surface aging of SZ2080 microstructures in conjunction with XPS measurements to correlate mechanical and chemical changes, and Minnick et al. [44], who focused on liquid-phase tensile testing of shape-memory microfibers, as further discussed in section 4.3.

The precision of AFM, however, comes with interpretative complexity. Elastic moduli extracted from Hertz, DMT, or JKR fits depend critically on tip shape, cantilever calibration, and the local Poisson's ratio (a parameter often uncertain for polymeric microstructures). Moreover, adhesion and hydration introduce long-range interactions that blur the classical notion of contact area. To mitigate these issues, current best practice involves in-situ calibration using reference samples of known moduli and combining AFM data with finite-element modeling of the tip–sample interaction. When applied to 2PL-fabricated PDMS and

IP-L780 resins, this approach yielded moduli within 10% of those obtained by nanoindentation, confirming AFM as both accurate and non-invasive when properly calibrated.

In summary, AFM-based mechanical characterization serves as a nanoscale complement to nanoindentation, extending mechanical quantification into lower-load, higher-resolution, and liquid-compatible regimes. It excels at revealing surface and interfacial phenomena—aging, adhesion, swelling, and phase separation—that govern the functionality of two-photon-polymerized structures but remain invisible to deeper-probing indentation. Its ability to map stiffness and dissipation alongside topography makes AFM a powerful nanomechanical imaging tool.

3.2 | Bulk Techniques

Although relatively straightforward in implementation, nanoindentation and AFM rely on mathematical models to extract mechanical properties—such as Young's modulus—from surface-level measurements. However, most mechanical properties relevant to practical applications are bulk quantities that surface techniques may not fully capture. To overcome this limitation, alternative characterization methods have been developed to study the bulk mechanical behavior of 2PL-fabricated materials.

3.2.1 | Micro-Tensile Testing

The mechanical characterization of structures fabricated by 2PL has long been dominated by microscale techniques, within a highly heterogeneous landscape ranging from AFM cantilevers and optical tweezers to micro-compression, nanoindentation, and other highly specialized approaches, yet tensile tests are particularly informative for assessing process stability. Koch et al. [102] highlighted that, compared with compression or indentation, these testing approaches are more sensitive to specimen defects such as microbubbles, microcracks, surface roughness, and notches, all of which are closely linked to system stability and polymerization parameters. For this reason, micro-tensile testing requires a dedicated discussion within the mechanical characterization of 2PL microstructures: it allows for a direct evaluation of the uniaxial response of the system and fundamental parameters such as Young's modulus, yield stress, ultimate tensile strength, and strain at failure.

From an experimental point of view, micro-tensile testing consists of applying a uniaxial load to a micro-specimen gripped at its ends by dedicated gripping systems. Throughout the test, the applied load and the elongation of the gauge section are recorded to derive the material stress–strain curve. Tensile tests are performed using dedicated micro- or nanomechanical systems and, in some cases, in situ inside a scanning electron microscope (SEM). This setup allows the specimen to be loaded until fracture, while the force is monitored by a load sensor and the deformation is either estimated from the gauge section displacement or precisely determined through digital image correlation.

From the stress–strain curve, Young's modulus, yield stress or yield onset, ultimate tensile strength, and strain at failure can be determined. The stress (σ) is calculated as the ratio between the applied load (F) and the initial cross-sectional area of the gauge section (A_0), whereas the strain (ε) is obtained by dividing the measured change in length (ΔL) by the initial gauge length (L_0). Young's modulus (E) is then derived from the slope of the initial linear elastic region of the stress–strain curve, while yield stress can be determined using the 0.2% offset criterion, and ultimate tensile strength corresponds to the maximum stress reached before fracture [124, 125]:

$$\sigma = \frac{F}{A_0}$$

$$\varepsilon = \frac{\Delta L}{L_0}$$

$$E = \frac{\sigma}{\varepsilon}$$

However, at the microscale, the accurate determination of the effective strain represents one of the most critical aspects of the test. Ideally, strain is derived from the change in length of the gauge section; in practice, in microtests, deformation cannot always be reliably obtained from actuator displacement alone, because the compliance of the system -including the gripper, the specimen head and base, as well as the substrate- all contribute to the measured response. As a result, the displacement values provided by the instrument may be affected by errors arising from the elastic deformation of the testing setup itself. To address this issue, several authors combine load measurement with digital image correlation (DIC), video tracking, or image-assisted deformation tracking in order to correct the effective elongation of the gauge section and obtain a more reliable estimate of the elastic modulus and the other mechanical parameters. Bauer et al. [125], for instance, reported that "the displacement was corrected for equipment and substrate compliances via a DIC algorithm," whereas Keckes et al. [124] showed that neglecting compliance correction may lead to an underestimation of the modulus by up to 30%. Minnick and co-workers [44] also used DIC to track both the deformation of the testing device and the actual deformation of the microfiber during tensile loading in liquid.

Beyond conventional mechanical parameters, micro-tensile testing can reveal deformation regimes and failure modes that depend on the geometry and topology of the structure. In particular, Moestopo et al. [126] showed that, in intertwined architectures, the tensile response may reveal distinct deformation pathways, including fiber alignment, fiber stretching, and knot tightening, which are associated with different values of failure strain and energy absorption.

A key aspect in micro-tensile testing is the possibility to carry out reliable measurements also in liquid environments, which is particularly relevant for the characterization of bio-based systems, hydrogels, and scaffolds. In the aforementioned work of Minnick et al. [44], a liquid-phase micro-tensile method for 2PL-fabricated microfibers was developed, explicitly showing that their mechanical behavior differs significantly from that measured in air. By employing DIC in this setup, the authors successfully tracked both the testing device displacement and the fiber length evolution during loading. This highlights that the mechanical response is highly sensitive to the testing environ-

ment, meaning that air-based measurements may not accurately reflect actual operating conditions.

As it will be clarified in Section 3.3, tensile characterization of 2PL structures has usually lacked standardized procedures, relying instead on procedures and protocols that vary between laboratories. This poses a significant challenge when materials, process parameters, and length scales need to be compared reliably. The mechanical behavior of 2PL materials cannot be reliably inferred or extrapolated from microscale tests alone, which makes standardized procedures especially relevant for industrial translation. Establishing standardized procedures is, therefore, a fundamental step for any real-world or industrial application of 2PL. The transition from microtests to uniaxial testing on larger specimens, however, is not straightforward. When component dimensions exceed the optical system's field of view, stitching multiple blocks becomes necessary, and the influence of these interfaces on the mechanical response must be carefully considered. In this context, Garcia-Taormina et al. [127] showed that scalability is a crucial challenge for 2PL structures and that stitch boundaries may introduce structural defects and non-uniformities capable of affecting the macroscopic mechanical behavior of the considered specimen. The same authors also highlighted that, due to print-volume limitations, the mechanical evaluation of these architectures has long been confined predominantly to compression tests, requiring both scaling-up strategies and testing methodologies to assess the effect of stitching on structural integrity under tensile loading.

In line with this issue, Forien et al. [128] showed that even nominally identical 2PL structures tested in tension at the millimeter scale may exhibit a wide scatter in elastic modulus, ultimate strength, and strain at failure; the authors discussed this variability in relation to printing defects and structural non-uniformities, including sub-lattice misalignment, resin shrinkage, laser beam shadowing, and local depletion of the oxygen inhibitor.

To overcome these limitations, Koch et al. [102] investigated materials compatible with upscaled 2PL, including the commercial resins UpPhoto and UpDraft, developed with this application in mind, and demonstrated for the first time the feasibility of performing ISO-standardized tests on 2PL-fabricated specimens of macroscopic dimensions.

3.2.2 | Other Static and Dynamic Bulk Testing Methods

Mechanical information on 2PL materials at the microscale might also be retrieved by exploiting deflection or inducing deformations periodically. One reported approach leveraging the flexural state of 2PL structures involves non-destructive bending tests on vertical micropillars produced using various photoresists (Figure 2C). By measuring the force required to achieve a predetermined displacement, researchers estimated material stiffness and demonstrated a direct correlation between Young's modulus and 2PL fabrication parameters, such as laser power [71]. The same method also shed light on the viscoelastic response of the materials. Understanding the time-dependent behavior of materials is particularly important when microstructures are subjected to long-term or cyclic loading. In such cases, dynamic mechanical testing is necessary, often requiring custom-built equipment. For example, Cayll et al. [129] developed a MEMS-based dynamic mechanical analysis (DMA) device utilizing a chevron-style thermal actuator. This setup allows 2PL microstructures to be directly fabricated on the device, which then applies tensile loads to the structures. The system achieved a displacement resolution of 1.5 ± 0.75 nm and a load resolution of 104 ± 52 nN, enabling the estimation of storage (G') and loss (G'') moduli of IP-Dip photoresist (Nanoscribe) across various temperatures and frequencies. The innovation of this approach lies in integrating conventional macroscopic testing principles with the specialized requirements of microscale structures fabricated via 2PL. The MEMS-based approach facilitates in situ testing, minimizes handling errors, and offers a robust platform for dynamic mechanical characterization.

Dynamic mechanical characterization techniques have also been exploited by Pertoldi et al. [66] to assess the elastic and damping properties of SZ2080. Frequency-dependent studies have yielded critical data on crosslinking density and overall structural integrity of this resist, enabling the estimation of the Young's modulus for this resist (Figure 2D).

In some cases, efforts to understand the mechanical behavior of 2PL-fabricated microstructures have driven the development of innovative characterization methodologies. One notable example is the work of Jelinek et al. [130], who adapted a nanoindentation system for tensile testing of micrometer-scale 2PL specimens. Their approach involved fabricating a double-edge-notched tension (DENT) structure within a push-to-pull frame. When compressed vertically by a nanoindenter tip, the frame deformed elastically, inducing tensile stress on the DENT specimen perpendicular to the indentation direction (Figure 2E). Upon fracture, the work of fracture could be accurately determined by decoupling the deformation contributions of the frame and the specimen in a force–displacement graph. This method enabled precise mechanical analysis and demonstrated scalability, paving the way for high-throughput testing platforms [131]. Moreover, insights from fracture analysis were instrumental in refining 2PL printing strategies (e.g., the introduction of slightly tapered geometries) to mitigate artifacts and imperfections in suspended structures without compromising mechanical integrity. This underscores the importance of mechanically informed design in enhancing the reliability and performance of microfabricated architectures.

Another sophisticated approach was developed by Minnick et al. [44], who employed AFM for uniaxial tensile testing on micrometer-scale specimens (Figure 2F). Their device featured two independent horizontally movable 2PL-fabricated structures—a sensing unit and an actuating unit—each supported by "A-shaped" vertical trusses and equipped with top stages. A micrometer-wide dog-bone sample (referred to as a microfiber) was printed between these two posts using the photoresist under investigation. Testing was initiated by anchoring an AFM probe to the actuating structure, which was then translated horizontally. The applied force transmitted through the microfiber caused a measurable deflection in the sensing structure, enabling accurate force determination, while strain in the microfiber was calculated from the relative displacement between the rest and the measuring positions. This setup enabled

precise measurement of Young's modulus and yield strength for photoresists such as IP-S and IP-Visio, supported loading–unloading cycles, and operated in liquid environments simulating physiological conditions. The method represents a significant advancement in microscale mechanical testing, combining high sensitivity, environmental versatility, and material-specific adaptability.

As a final example of original characterization methods, we report the introduction of laser-based dynamic vibrational testing, which was recently proposed by Kai and colleagues [132]. The authors exploit the photoacoustic excitation of elastic waves on the surface of metamaterials fabricated via 2PL, showing different architectures, to achieve stiffness values compatible to those obtained with indentation-based techniques without destroying the structures. The technique also showed its potential to identify defects in the metamaterial structure.

Collectively, these investigations underscore the importance of integrating dynamic, static, and in situ testing methodologies to achieve a comprehensive understanding of the structure–property relationships governing material performance at the microscale. The ongoing evolution of mechanical characterization—driven by innovations in high-throughput platforms, MEMS-based analyzers, and computational modeling—ensures rigorous evaluation of even the most intricate microfabricated structures. Notably, the cross-disciplinary synthesis of insights has led to the development of predictive models that deepen our understanding of material behavior and guide the design of more reliable and efficient microdevices. As the field advances, these integrated, predictive approaches are poised to become the gold standard for mechanical characterization in emerging technological applications.

3.3 | The Quest for Standardization

These approaches highlight the critical need for a reliable estimation of mechanical properties in 2PL-fabricated materials and structures. However, a major barrier to the industrial adoption of 2PL remains the lack of systematic data on material properties and the limited understanding of their correlation with processing parameters. Despite the availability of numerous characterization techniques, a standardized metrological framework for 2PL is still missing [133]. The importance of this gap is evident from findings that different nanoindentation protocols can yield significantly different mechanical properties for the same material under identical polymerization conditions [104].

To address this gap, Cantoni et al. [134] conducted a round-robin study to compare polymerization accuracy and geometric fidelity across different commercially available 2PL systems. Their investigation included diverse conditions—free-hanging geometries, stitching, and multi-scale structures—using the three most widely used commercial 2PL platforms. While the study offered valuable insights into the capabilities and limitations of each system, it did not assess the mechanical properties of the fabricated structures. Surface characterization was limited to AFM-measured root-mean-square roughness (Rq), and different photoresists were used for each system, complicating direct comparisons. Nevertheless, this work marks a significant milestone toward standardization in 2PL, laying the groundwork for future studies integrating mechanical performance metrics into comparative analyses.

Indeed, material properties could be measured on macroscopic specimens: fabrication times of macroscopic structures can be reduced by using lower-magnification objectives, albeit at the cost of decreased resolution [135]. It should be noted that structures produced with low-magnification objectives may not exhibit identical mechanical properties to those obtained via higher-magnification objectives, in principle. Indeed, voxel dimensions and proximity effects (e.g., Schwarzschild effect, shadowing of already polymerized material, photoresist shrinkage) [136–140] can affect structural continuity, leading to scale-dependent variations in measured properties. Similarly, mechanical properties measured on macroscopic specimens might not be directly applicable to structures at the microscale. Indeed, several factors, including possible polymerization-induced defects, size effects, and stress localization, can lead to significant differences in micromechanical properties [141, 142]. However, the potential of carrying out a systematic investigation of the mechanical response of specimens from the micro- to the macroscale was demonstrated recently [102]. As discussed above, Koch et al. leveraged the reduced fabrication time which can be achieved not only by modulating the writing speed, but also by using objectives at lower magnification in combination with adaptive resolution ("coarse mode," which increases voxel dimensions and thereby volumetric build rates) to fabricate standardized macroscopic specimens. Once the writing parameters (e.g., slicing and hatching of adjacent voxel lines) are optimized for a given material, specimens of 2–20 mm (e.g., dog-bone specimens) can be fabricated for testing with conventional mechanical characterization equipment, such as tensile testers, hardness indenters, and three-point bending setups. Such standardized cross-scale testing is essential for evaluating the application potential of newly developed 2PL materials and for ensuring process stability. However, not all photoresists compatible with 2PL may be processable at high writing speeds, potentially limiting the feasibility of macroscopic specimen fabrication. Besides using lower magnification objectives, other strategies to increase fabrication speed were commercialized (e.g., galvanometric mirrors to complement the motion of piezoelectric stages on which the sample is placed) or developed [143–145], but the possibility of realizing structures at the macroscale with resolution typical of 2PL systems in reasonable time remains a partially unaccomplished challenge, which would clearly improve -among others- our capability to investigate the mechanical features of the used photoresists. Another strategy to obtain standardizable stiffness measurements, proposed by Bauer et al. [125], involves developing an empirical model correlating 2PL writing parameters with the degree of crosslinking and, consequently, with Young's modulus. Initially developed for IP-Dip and requiring the determination of material-specific constants, the model is expected to apply to other acrylate-based resists and, potentially, to any photo-crosslinkable material used in 2PL. Key input parameters include hatching distance, laser power, and the optical characteristics of the 2PL system.

Recently, Eivgi et al. [104] summarized the best practices for nanoindentation characterization to ensure accurate and trustworthy Young's modulus determination for 2PL resins.

In summary, significant theoretical and practical efforts are underway to standardize protocols and procedures in 2PL fabrication. Emerging methodologies aim to reduce reliance on custom setups and establish universal, predictive models for the mechanical properties of 2PL materials, accelerating their integration into industrial and technological applications.

4 | Mechanical Properties as Functional Features in Static and Dynamic 2PL Structures

Historically, the mechanical characterization of 2PL-fabricated microstructures has primarily served to elucidate the influence of polymerization parameters on material behavior. In this context, mechanical testing has been instrumental in deepening our understanding of the 2PL process itself, resulting in a substantial dataset detailing the key mechanical properties of commonly used photoresists.

However, as novel materials for 2PL continue to emerge, researchers have increasingly recognized that the potential of the technology lies not only in its ability to fabricate unprecedentedly complex 3D geometries with sub-micrometer resolution, but also in its capacity to finely tune mechanical properties for functional applications. This shift in perspective has led to the design of an expanding array of microstructures in which geometry, material composition, and structural characteristics are synergistically engineered to achieve innovative functionalities across diverse fields.

4.1 | Cell (Mechano)Biology

Disentangling the respective contributions of 3D architecture and material properties to biological responses is often challenging. Nevertheless, the literature provides a substantial subset of studies where the mechanical features of 3D structures can be clearly linked to specific cellular behavior or biological properties.

One of the earliest landmark examples is the work of Klein et al. [146], who developed spiderweb-like 3D structures composed of suspended beams that could be deflected by forces of approximately 50 nN. Measuring the force–displacement behavior of these beams—directly related to their stiffness—enabled, for the first time, an accurate estimation of forces exerted by single cells in a 3D scaffold. Building on this concept, the exploitation of flexural properties in acrylate-based 3D structures has led to several biologically relevant findings, including (i) an inverse correlation between breast cancer cell invasiveness and materials stiffness [38, 147], (ii) actin cytoskeleton remodeling induced by controlled cyclic mechanical stimulation at 0.5 Hz of human fibroblast-like synoviocytes (HFLS) and human umbilical vein endothelial cells (HUVEC) on a multimaterial 2PL scaffold [148], (iii) increased mineralization (i.e., increased calcium and phosphorus deposition) by osteoblast-like SAOS-2 cells cultured on soft tetrakaidekahedral lattice scaffolds (E = 0.7 MPa) compared to stiff ones (E = 100 MPa) [69] (Figure 3A). Stimuli-responsive 2PL scaffolds have also enabled researchers to gain insights into the mechanisms underlying cell force response: for example, a rapid increase (within 30 min) in traction forces induced by the controlled swelling of a concentration-responsive photoresist [29] was observed for osteosarcoma cells (U2OS) and NIH3T3 fibroblasts. This behavior was shown to be reversible when traction is released, unless non-muscle myosin IIA (nmMIIA) was pharmacologically inhibited or nmMIIA knock-out cell lines were used, suggesting that cellular tensional homeostasis strongly depends on functional myosin motors (Figure 3B). 2PL-based 3D structures have demonstrated their potential in investigating the mechanics of biological systems, also in the presence of stem cells and primary cells: indeed, enhanced neurite directionality was demonstrated in primary hippocampal neurons and neural progenitor cells in response to low shear modulus in the range 0.5–35 MPa [46] (Figure 3C). More recently, Lodhi et al. [149] advanced cell force sensing applications by integrating piezoresistive elements beneath 2PL-fabricated flexible micropillars. These structures enabled highly accurate and sensitive force measurements based on pillar deflection induced by cellular mechanical activity.

4.2 | Metamaterials

The term "metamaterials" originally referred to materials exhibiting unusual electromagnetic properties, such as a negative refractive index. Today, it more broadly denotes materials with extraordinary or rare mechanical properties, achieved through carefully engineered micro- or nano-architectures. While the distinctive features of metamaterial classes have been widely reviewed elsewhere [150, 151], here we focus on examples of micro- and mesostructures where the key interest lies not in the exotic "meta" behavior per se, but in how their unique mechanical characteristics enable other scientific applications.

Within this category, notable examples include meta-biomaterials, photonic metamaterials, and metasurfaces. Rationally designed meta-biomaterials, specifically characterized by auxeticity (i.e., a negative Poisson's ratio), have been developed to serve mechanobiology and tissue engineering purposes [152]. Leveraging the extremely high resolution of 2PL, intricate structures featuring different lattice geometries have been interfaced with fibroblasts [153, 154], bone stem cells [155], and mesenchymal stem cells [156] (Figure 3D). In these works, both the scaffold design and its mechanical properties directly influenced cell colonization, differentiation, and force generation. However, a universal consensus on the role of Poisson's ratio or auxeticity on cell fate remains elusive, as these effects are intrinsically linked to other scaffold properties (e.g., Young's modulus, porosity, etc.) and because most investigations were performed under static conditions, without dynamic loading.

Beyond biomedical engineering, 2PL-fabricated microstructures also play a pivotal role in photonics and metasurface applications. Recently, neuron-inspired metastructures [157] have opened new avenues for creating low-density 3D materials with applications in light-matter interactions and 3D topological photonics. 2PL also enabled the manufacturing of multilevel metalenses [158], with numerical apertures up to 0.96, which play a crucial role in enhancing light-matter interaction mechanisms. An instructive example of the correlation between metamaterials' mechanical features and optical properties resides in the work of Choi and co-workers [159]: here, the geometry of the helical pattern

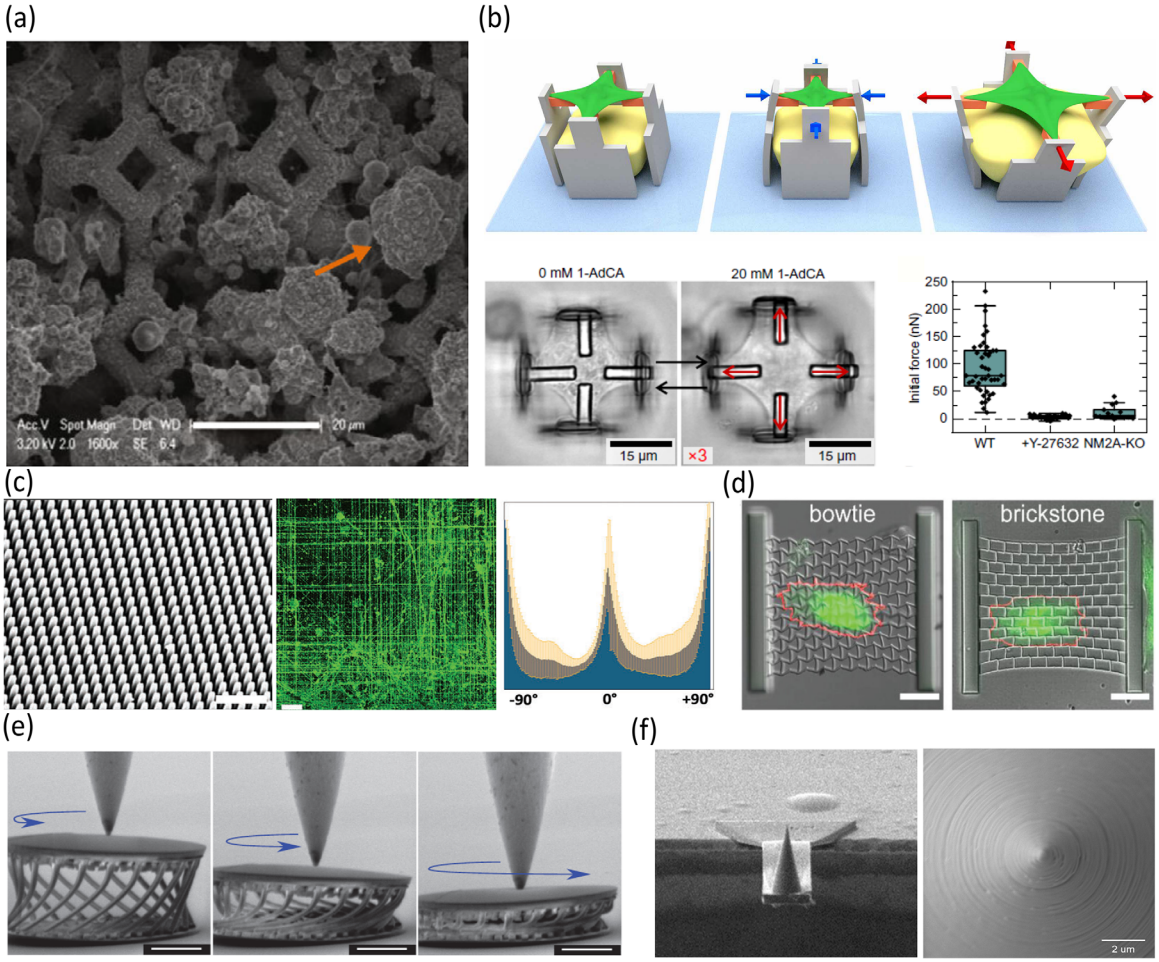

FIGURE 3 | Relevance of mechanical properties of 2PL materials and structures for functional investigations. Panel (a): on soft 3D nanolattices, osteoblast-like cells showed increased mineral secretions and intracellular f-actin and vinculin concentrations with respect to cells cultured o stiffer structures with similar geometry (adapted with permission [69] Copyright 2017, Elsevier; panel (b): single-cell stretching induced by structure deflection shows that cellular tensional homeostasis strongly depends on functional myosin motors (adapted with permission [29] Copyright 2020, Wiley; panel (c): the shear modulus of nanopillar arrays correlates with the growth directionality of hippocampal neurons (adapted with permission [46] Copyright 2024, Wiley; panel (d): morphometric parameters of human mesenchymal stem cells, such as the projected area per cell and the aspect ratio, show clear differences across 2PLL metamaterial structures (adapted with permission [156]. Copyright 2024, Wiley; panel (e): design optimization of metamaterials via machine learning leads to supercompressible 3D microstructures (adapted with permission [160]. Copyright 2019, Wiley; panel (f): AFM cantilever and tip fabricated via 2PL (adapted with permission [163]. Copyright 2024, MDPI).

was carefully calibrated to confer architectural and mechanical stability to the fabricated microstructures, which in turn affects the chiroptical properties. Additionally, the authors managed to embed the micro-coils in PDMS and to control the response in ellipticity when subjected to compressive load.

Finally, in recent years, synergistic approaches of machine learning-driven design and 2PL microfabrication have led to the realization of barrel-shaped [160] or dome-like [161] deformable structures showing unprecedented flexibility (Figure 3E).

4.3 | Exploiting Mechanical Properties for Opto-Acoustic Sensing and Highly Precise Manufacturing

Partially overlapping with the metamaterials domain, the work of Stinson and collaborators explores the compression properties of 2PL photoresists—specifically IP-Dip—for developing tunable beam splitters and micromechanical sensors [162] (Figure 3F). Although the functionality of the fabricated 3D structures was not experimentally demonstrated, numerical simulations assessed the opto-mechanical behavior of an array of slanted wires operating in the infrared spectral range. The slanted-wire grating geometry was designed to modulate transmitted diffraction order efficiencies as a function of the slant angle φ, which could be dynamically adjusted through mechanical compression. Simulations indicated that slant angle variations between 35° and 45° could be achieved with compression forces in the millinewton range, suggesting that the fabricated pillars are sufficiently compliant to produce measurable changes in diffraction efficiency.

Beyond optical applications, the acoustic properties of 3D structures have also been investigated in relation to their mechanical characteristics. In a preliminary study, scanning acoustic

microscopy was combined with nanoindentation to correlate the acoustic impedance of 500 × 500 × 100 μm^3 cuboids—fabricated using the IP-Q photoresist—with their elastic modulus. The estimated impedance, approximately 3.5 MRayl within the MHz frequency range, was found to be directly influenced by the laser power used during fabrication. These insights open promising avenues for optimizing material compositions and geometries in the development of functional acoustic metamaterials.

In a particularly innovative application, Gaso et al. [163] successfully designed and fabricated AFM cantilevers and tips using IP-Dip photoresist. By integrating previously measured Young's modulus values with theoretical models, they estimated the resonant frequencies of the probes, which were subsequently employed to detect surface topographies with nanometric resolution. Their results highlight the excellent performance of these cantilevers for high-resolution imaging and precise surface characterization over large areas. Moreover, this work demonstrates the feasibility of using 2PL-fabricated structures not only for imaging but also for mechanical investigations of other 2PL architectures. This expands the scope of AFM-related techniques in conjunction with 2PL, including advanced methods such as dip-pen nanolithography and Microchannel Cantilever Spotting [164].

Alongside functional device fabrication, ensuring the structural integrity of 3D architectures represents a fundamental yet often overlooked objective. Fine control over the final geometry at a nanometer scale has been achieved only in a few recent works, but it is essential for guaranteeing uniform mechanical properties throughout the structure. Although this may appear secondary due to its lack of immediate applications, refining 2PL polymerization strategies could unlock new design possibilities and enhance the functionality of existing devices. For instance, in the metamaterials field, the fidelity of the fabricated outcome to the intended design is critical: Kurpiers et al. [80] demonstrated that continuous nonlinear variations in laser power during writing result in nanometric adjustments of the designed geometries in tetrahedral lattices. In particular, joints between adjacent beams were modified from rounded shapes to sharp notches, and beams with convex and concave shapes were realized. This not only increases design freedom for mechanical metamaterials, but also impacts the control over imperfections in fabrication, which were considered unavoidable.

Efforts to minimize mismatches between design and fabrication results have also been reported by Oguguo et al. [165], who introduced compensation factors to counteract distortion sources in voxel polymerization—such as defocusing, voxel size, and proximity effects—when designing gyroid-like and lattice structures. Unaddressed fabrication inaccuracies can lead to inconsistencies in 3D structures and poor mechanical response, even when the dimensions of the realized specimens are macroscopic. Several authors report that overcoming fabrication defects to achieve predictable mechanical behavior cannot be accomplished solely by refining the design of the intended architectures [128]. In such cases, a comprehensive rethinking of both the materials —e.g., by introducing resins with better mechanical performance [50]— and the 2PL process parameters is required.

5 | Conclusions

Two-photon lithography (2PL) has emerged as a transformative technology in high-resolution additive manufacturing, enabling precise fabrication at the micro- and nanoscale. The mechanical properties of 2PL structures—such as Young's modulus, Poisson's ratio, fracture toughness, and viscoelastic response—cannot be regarded as fixed attributes of a given resin. Instead, they result from a complex interplay of resin chemistry, printing parameters, environmental conditions, and post-processing treatments. Understanding and controlling these properties is essential for ensuring the structural integrity, functionality, and long-term reliability of 2PL-fabricated devices. Acrylate-based resins, including commercial formulations, dominate the field due to their high stiffness and strength. However, custom resin formulations usually offer flexibility in tailoring properties. Notably, stiffness can vary by an order of magnitude depending on fabrication conditions: higher laser power, slower scan speeds, and denser slicing and hatching generally increase crosslink density and modulus. Post-processing methods such as UV curing and thermal annealing can be used to enhance rigidity, while emerging "4D materials"—structures designed to change shape or stiffness in response to external stimuli—introduce dynamic mechanical behaviors.

Taken together, these considerations suggest that the versatility of 2PL over other microfabrication techniques lies not only in the virtually unrestricted capability to create free-form 3D geometries, but also in the possibility of selecting among a variety of photoresists and processing strategies the most suitable to achieve the desired mechanical features for the intended application. Advanced characterization techniques, computational modeling, and post-processing treatments have greatly refined our understanding of how process variables influence material outcomes at both the micro- and nanoscale.

As the number of 2PL structures continues to grow, several emerging directions can be envisioned for the field. The development of complex materials—including nanocomposites, hybrid organic–inorganic formulations, and functional hydrogels—promises tunable mechanical, chemical, and biological properties. The integration of real-time mechanical characterization within fabrication workflows could enable adaptive printing, reducing trial-and-error and improving reproducibility. Predictive design approaches leveraging multiphysics modeling and machine learning may soon forecast mechanical performance based on resin chemistry, exposure settings, and geometry, accelerating innovation.

The future of 2PL will also depend on treating mechanical properties as fundamental design parameters, along with geometric and optical considerations. As micro- and nanoscale devices become increasingly integral to biomedical research, industry, and healthcare, the demand for robust, predictable mechanical behavior will intensify. Reliable microfluidic platforms, bioengineered tissues, soft robots, and tunable metamaterials will require not only dimensional precision but also carefully engineered elasticity, toughness, and dynamic response. By emphasizing mechanical understanding alongside geometric control, 2PL can truly emerge as a key enabling technology for advanced manufacturing,

transitioning from empirical, proof-of-concept approaches to data-driven, predictive workflows at higher technology readiness levels.

Author Contributions

Edoardo Rossi: investigation, writing – original draft, writing – review and editing. **Edoardo Bemporad**: writing – original draft, writing – review and editing, supervision. **Dalila Fontana**: conceptualization, investigation, writing – original draft, writing – review and editing. **Alberto Rainer**: investigation, writing – original draft, writing – review and editing, funding acquisition, supervision. **Enrico D. Lemma**: conceptualization, investigation, writing – original draft, writing – review and editing, funding acquisition, supervision. **Angelo Accardo**: writing – original draft, writing – review and editing, investigation, supervision. **Marco Sebastiani**: writing – original draft, writing – review and editing, supervision.

Acknowledgements

This work was supported by the Italian Ministry of Research, under the complementary actions to the NRRP "Fit4MedRob—Fit for Medical Robotics" Grant (# PNC0000007). This work was also funded by the European Union—Next Generation EU, Italian NRRP M4.C2—Investment 1.5 "Rome Technopole", CUP C83C22000510001. E.D.L. acknowledges the Italian Ministry for University and Research (FIS Starting Grant, CUP: C53C25001050001).

Open access publishing facilitated by Universita Campus Bio-Medico di Roma, as part of the Wiley - CRUI-CARE agreement.

Conflicts of Interest

The authors declare no conflicts of interest.

Data Availability Statement

The data that support the findings of this study are available from the corresponding author upon reasonable request.

References

1. H. Wang, W. Zhang, D. Ladika, et al., "Two-Photon Polymerization Lithography for Optics and Photonics: Fundamentals, Materials, Technologies, and Applications," *Advanced Functional Materials* 33 (2023): 2214211, https://doi.org/10.1002/adfm.202214211.

2. M. Marini, A. Nardini, R. Martínez Vázquez, et al., "Microlenses Fabricated by Two-Photon Laser Polymerization for Cell Imaging With Non-Linear Excitation Microscopy," *Advanced Functional Materials* 33 (2023): 2213926, https://doi.org/10.1002/adfm.202213926.

3. O. Vanderpoorten, Q. Peter, P. K. Challa, et al., "Scalable Integration of Nano-, and Microfluidics With Hybrid Two-photon Lithography," *Microsystems and Nanoengineering* 5 (2019): 40, https://doi.org/10.1038/s41378-019-0080-3.

4. A. Marino, O. Tricinci, M. Battaglini, et al., "A 3D Real-Scale, Biomimetic, and Biohybrid Model of the Blood-Brain Barrier Fabricated through Two-Photon Lithography," *Small* 14 (2018): 1702959, https://doi.org/10.1002/smll.201702959.

5. A. Ruggiero, V. Criscuolo, S. Grasselli, et al., "Two-photon Polymerization Lithography Enabling the Fabrication of PEDOT:PSS 3D Structures for Bioelectronic Applications," *Chemical Communications* 58 (2022): 9790–9793, https://doi.org/10.1039/D2CC03152C.

6. B. N. L. Costa, A. Marote, C. Barbosa, J. Campos, A. J. Salgado, and J. B. Nieder, "Smart Polymeric 3D Microscaffolds Hosting Spheroids for Neuronal Research via Quantum Metrology," *Advanced Healthcare Materials* 14 (2025): 2403875, https://doi.org/10.1002/adhm.202403875.

7. T. Frenzel, M. Kadic, and M. Wegener, "Three-dimensional Mechanical Metamaterials With a Twist," *Science (1979)* 358 (2017): 1072.

8. L. Wang, G. Ulliac, B. Wang, et al., "3D Auxetic Metamaterials with Elastically-Stable Continuous Phase Transition," *Advanced Science* 9 (2022): 2204721, https://doi.org/10.1002/advs.202204721.

9. K. Weißenbruch, E. D. Lemma, M. Hippler, and M. Bastmeyer, "Microscaffolds as Synthetic Cell Niches: Recent Advances and Challenges," *Current Opinion in Biotechnology* 73 (2022): 290–299, https://doi.org/10.1016/j.copbio.2021.08.016.

10. M. Hippler, E. D. Lemma, S. Bertels, et al., "3D Scaffolds to Study Basic Cell Biology," *Advanced Materials* 31 (2019): 1808110, https://doi.org/10.1002/adma.201808110.

11. C. Greant, B. Van Durme, J. Van Hoorick, and S. Van Vlierberghe, "Multiphoton Lithography as a Promising Tool for Biomedical Applications," *Advanced Functional Materials* 33 (2023): 2212641, https://doi.org/10.1002/adfm.202212641.

12. W. Xie, X. Wei, H. Kang, et al., "Static and Dynamic: Evolving Biomaterial Mechanical Properties to Control Cellular Mechanotransduction," *Advanced Science* 10 (2023): 2204594, https://doi.org/10.1002/advs.202204594.

13. P. Mainik, C. A. Spiegel, and E. Blasco, "Recent Advances in Multi-Photon 3D Laser Printing: Active Materials and Applications," *Advanced Materials* 36 (2024): 2310100, https://doi.org/10.1002/adma.202310100.

14. L. Florea, E. Blasco, and V. Mattoli, "New Frontiers in Materials and Technologies for 3D Two Photon Polymerization," *Advanced Functional Materials* 33 (2023): 2305697, https://doi.org/10.1002/adfm.202305697.

15. A. Jaiswal, C. K. Rastogi, S. Rani, G. P. Singh, S. Saxena, and S. Shukla, "Two decades of two-photon lithography: Materials science perspective for additive manufacturing of 2D/3D nano-microstructures," *iScience* 26 (2023): 106374.

16. S. F. Liu, Z. W. Hou, L. Lin, Z. Li, and H. B. Sun, "3D Laser Nanoprinting of Functional Materials," *Advanced Functional Materials* 33 (2023): 2211280, https://doi.org/10.1002/adfm.202211280.

17. S. O'Halloran, A. Pandit, A. Heise, and A. Kellett, "Two-Photon Polymerization: Fundamentals, Materials, and Chemical Modification Strategies," *Advanced Science* 10 (2023): 2204072, https://doi.org/10.1002/advs.202204072.

18. M. Carlotti and V. Mattoli, "Functional Materials for Two-Photon Polymerization in Microfabrication," *Small* 1902687 (2019): 1.

19. P. Golvari and S. M. Kuebler, "Fabrication of functional microdevices in su-8 by multi-photon lithography," *Micromachines (Basel)* 12 (2021): 472, https://doi.org/10.3390/mi12050472.

20. L. Brigo, A. Urciuolo, S. Giulitti, et al., "3D high-resolution two-photon crosslinked hydrogel structures for biological studies," *Acta Biomaterialia* 55 (2017): 373–384, https://doi.org/10.1016/j.actbio.2017.03.036.

21. A. E. Chalard, A. W. Dixon, A. J. Taberner, and J. Malmström, "Visible-Light Stiffness Patterning of GelMA Hydrogels towards in Vitro Scar Tissue Models," *Frontiers in Cell and Developmental Biology* 10 (2022): 946754, https://doi.org/10.3389/fcell.2022.946754.

22. G. Menassol, B. van der Sanden, L. Gredy, et al., "Gelatine–collagen photo-crosslinkable 3D matrixes for skin regeneration," *Biomaterials Science* (2024): 1738–1749, https://doi.org/10.1039/d3bm01849k.

23. H. Fu and B. Yu, "3D micro/Nano Hydrogel Structures Fabricated by Two-photon Polymerization for Biomedical Applications," *Frontiers in Bioengineering and Biotechnology* 12 (2024): 1–11, https://doi.org/10.3389/fbioe.2024.1339450.

24. X. Li, H. Wang, X. Dong, et al., "Accurate Modulation of Photoprinting Under Stiffness Imaging Feedback for Engineering ECMs With High-fidelity Mechanical Properties," *Microsystems & Nanoengineering* 8 (2022): 60, https://doi.org/10.1038/s41378-022-00394-y.

25. F. Valente, M. S. Hepburn, J. Chen, et al., "Bioprinting Silk Fibroin Using Two-photon Lithography Enables Control Over the Physico-

chemical Material Properties and Cellular Response," *Bioprinting* 25 (2022): e00183, https://doi.org/10.1016/j.bprint.2021.e00183.

26. Q. Duan, W. C. Zhang, J. Liu, et al., "22 nm Resolution Achieved by Femtosecond Laser Two-Photon Polymerization of a Hyaluronic Acid Vinyl Ester Hydrogel," *ACS Applied Materials & Interfaces* 15 (2023): 26472–26483, https://doi.org/10.1021/acsami.3c04346.

27. H. Yu, H. Ding, Q. Zhang, Z. Gu, and M. Gu, "Three-Dimensional Direct Laser Writing of PEGda Hydrogel Microstructures With Low Threshold Power Using a Green Laser Beam," *Light: Advanced Manufacturing* 2 (2021): 31–38, https://doi.org/10.37188/lam.2021.003.

28. M. Belqat, X. Wu, L. P. C. Gomez, et al., "Tuning Nanomechanical Properties of Microstructures Made by 3D Direct Laser Writing," *Addit Manuf* 47 (2021): 102232, https://doi.org/10.1016/j.addma.2021.102232.

29. M. Hippler, K. Weißenbruch, K. Richler, et al., "Mechanical Stimulation of Single Cells by Reversible Host-Guest Interactions in 3D Microscaffolds," *Science Advances* 6 (2020): abc2648.

30. E. Yarali, A. A. Mubeen, K. Cussen, et al., "Two-photon Polymerization Based 4D Printing of Poly(N-isopropylacrylamide) Hydrogel Microarchitectures for Reversible Shape Morphing," *Scientific Reports* 15 (2025): 21549, https://doi.org/10.1038/s41598-025-06269-2.

31. P. F. J. van Altena, L. Castillo Ransanz, M. Manco, V. M. Heine, and A. Accardo, "Micro-digital Light Processing of Conventional and Hollow Gyroid Mesoscale Hydrogel Scaffolds for Neural Cell Cultures," *Micro and Nano Engineering* 28 (2025): 100310, https://doi.org/10.1016/j.mne.2025.100310.

32. D. Song, A. Husari, F. Kotz-Helmer, P. Tomakidi, B. E. Rapp, and J. Rühe, "Two-Photon Direct Laser Writing of 3D Scaffolds Through C, H-Insertion Crosslinking in a One-Component Material System," *Small* 20 (2024): 2306682, https://doi.org/10.1002/smll.202306682.

33. W. Qiu, M. Bernero, M. E. Ye, et al., "A Water-Soluble PVA Macrothiol Enables Two-Photon Microfabrication of Cell-Interactive Hydrogel Structures at 400 Mm s^{-1}," *Advanced Materials* 38 (2026): 10834, https://doi.org/10.1002/adma.202510834.

34. P. Mainik, C. A. Spiegel, J. L. G. Schneider, M. Wegener, and E. Blasco, "Deep Eutectic Inks for Multiphoton 3D Laser Microprinting," *Advanced Materials* 37 (2025): 2507640, https://doi.org/10.1002/adma.202507640.

35. T. N. Eren, J. Liang, J. L. G. Schneider, et al., "Soft and Stiff 3D Microstructures by Step-Growth Photopolymerization Using a Single Photoresin and Multi-Photon Laser Printing," *Advanced Functional Materials* 36 (2025): 2502876, https://doi.org/10.1002/adfm.202502876.

36. X. Yang, Y.-F. Niu, M.-X. Wei, et al., "Generating Microstructures With Highly Variable Mechanical Performance Using Two-Photon Lithography and Thiol-ene Photopolymerization," *Chinese Journal of Polymer Science* 41 (2023): 67–74, https://doi.org/10.1007/s10118-022-2802-5.

37. B. Zhao, J. Li, X. Yang, S. He, X. Pan, and J. Zhu, "Degradable 3D Printed Objects With Tunable Mechanical Properties via Photoinduced Free Radical Promoted Cationic RAFT Polymerization," *ACS Applied Polymer Materials* 6 (2024): 1584–1591, https://doi.org/10.1021/acsapm.3c03164.

38. E. D. Lemma, S. Sergio, B. Spagnolo, et al., "Tunable Mechanical Properties of Stent-Like Microscaffolds for Studying Cancer Cell Recognition of Stiffness Gradients," *Microelectronic Engineering* 190 (2018): 11–18, https://doi.org/10.1016/j.mee.2018.01.007.

39. L. Zheng, H. Liang, J. Tang, et al., "Micrometer-scale Poly(ethylene glycol) With Enhanced Mechanical Performance," *Nature Communications* 16 (2025): 4391, https://doi.org/10.1038/s41467-025-59742-x.

40. P. F. J. van Altena and A. Accardo, "Micro 3D Printing Elastomeric IP-PDMS Using Two-Photon Polymerisation: A Comparative Analysis of Mechanical and Feature Resolution Properties," *Polymers (Basel)* 15 (2023): 1816, https://doi.org/10.3390/polym15081816.

41. R. Srinivasaraghavan Govindarajan, S. Sikulskyi, Z. Ren, T. Stark, and D. Kim, "Characterization of Photocurable IP-PDMS for Soft Micro Systems Fabricated by Two-Photon Polymerization 3D Printing," *Polymers (Basel)* 15 (2023): 4377, https://doi.org/10.3390/polym15224377.

42. Nanoscribe GmbH, Technical Brochure (2026).

43. M. Diamantopoulou, N. Karathanasopoulos, and D. Mohr, "Stress-strain Response of Polymers Made Through Two-photon Lithography: Micro-scale Experiments and Neural Network Modeling," *Additive Manufacturing* 47 (2021): 102266, https://doi.org/10.1016/j.addma.2021.102266.

44. G. Minnick, B. T. Safa, J. Rosenbohm, et al., "Two-Photon Polymerized Shape Memory Microfibers: A New Mechanical Characterization Method in Liquid," *Advanced Functional Materials* 33 (2023): 2206739, https://doi.org/10.1002/adfm.202206739.

45. N. Rohbeck, R. Ramachandramoorthy, D. Casari, et al., "Effect of High Strain Rates and Temperature on the Micromechanical Properties of 3D-printed Polymer Structures Made by Two-photon Lithography," *Materials & Design* 195 (2020): 108977, https://doi.org/10.1016/j.matdes.2020.108977.

46. G. Flamourakis, Q. Dong, D. Kromm, et al., "Deciphering the Influence of Effective Shear Modulus on Neuronal Network Directionality and Growth Cones' Morphology via Laser-Assisted 3D-Printed Nanostructured Arrays," *Advanced Functional Materials* 35 (2024): 2409451, https://doi.org/10.1002/adfm.202409451.

47. UpNano GmbH, Technical Brochure (2026).

48. IQS NANO, Technical Brochure (2026).

49. MicroResist Technology GmbH, Technical Brochure (2026).

50. J. Hu, Y. Gao, L. Wu, et al., "High Performance Two Photon Polymerization Resin Designed for Sub-micron Precision and Millimeter Scale Structure Manufacturing," *Chemical Engineering Journal* 505 (2025): 159194, https://doi.org/10.1016/j.cej.2024.159194.

51. T. Ritacco, W. Di Cianni, D. Perziano, et al., "High-Resolution 3D Fabrication of Glass Fiber-Reinforced Polymer Nanocomposite (FRPN) Objects by Two-Photon Direct Laser Writing," *ACS Applied Materials & Interfaces* 14 (2022): 17754–17762, https://doi.org/10.1021/acsami.1c21708.

52. D. Schwärzle, X. Hou, O. Prucker, and J. Rühe, "Polymer Microstructures Through Two-Photon Crosslinking," *Advanced Materials* 29 (2017): 1703469, https://doi.org/10.1002/adma.201703469.

53. M. Buzio, M. Gini, T. C. Schneider, et al., "micropatterning of PEDOT:PSS/Gelatin Conductive Hydrogels via Two-photon Lithography for Soft ," *Bioelectronicsnpj Flexible Electronics* 10 (2026): 19, https://doi.org/10.1038/s41528-026-00529-5.

54. K. M. Lichade, S. Shiravi, J. D. Finan, and Y. Pan, "Direct Printing of Conductive Hydrogels Using Two-photon Polymerization," *Addit Manuf* 84 (2024): 104123, https://doi.org/10.1016/j.addma.2024.104123.

55. C. Amruth, A. K. Singh, A. Sharma, D. Corzo, and D. Baran, "Micro-3D Printed Conductive Polymer Composite via Two-Photon Polymerization for Sensing Applications," *Advanced Materials Technologies* 9 (2024): 2400290, https://doi.org/10.1002/admt.202400290.

56. X. Zhou, X. Liu, and Z. Gu, "Photoresist Development for 3D Printing of Conductive Microstructures via Two-Photon Polymerization," *Advanced Materials* 36 (2024): 2409326, https://doi.org/10.1002/adma.202409326.

57. Z. Dong, J. Monti, H. Cui, et al., "Material-Independent 3D Patterning Via Two-Photon Lithography and Discontinuous Wetting," *Advanced Materials Technologies* 8 (2023): 2201268, https://doi.org/10.1002/admt.202201268.

58. M. Dong, X. Wang, X. Z. Chen, et al., "D-Printed Soft Magnetoelectric Microswimmers for Delivery and Differentiation of Neuron-Like Cells," *Advanced Functional Materials* 30 (2020): 1910323, https://doi.org/10.1002/adfm.201910323.

59. K. Liu, H. Ding, S. Li, et al., "3D printing Colloidal Crystal Microstructures via Sacrificial-scaffold-mediated Two-photon Lithography," *Nature Communications* 13 (2022): 4563, https://doi.org/10.1038/s41467-022-32317-w.

60. H. Lee, D. Kim, S. Kwon, and S. Park, "Magnetically Actuated Drug Delivery Helical Microrobot With Magnetic Nanoparticle Retrieval Ability," *ACS Applied Materials & Interfaces* 13 (2021): 19633–19647, https://doi.org/10.1021/acsami.1c01742.

61. H. Ceylan, I. C. Yasa, O. Yasa, A. F. Tabak, J. Giltinan, and M. Sitti, "3D-Printed Biodegradable Microswimmer for Theranostic Cargo Delivery and Release," *ACS Nano* 13 (2019): 3353–3362, https://doi.org/10.1021/acsnano.8b09233.

62. S. Ushiba, S. Shoji, K. Masui, P. Kuray, J. Kono, and S. Kawata, "3D microfabrication of Single-wall Carbon Nanotube/Polymer Composites by Two-photon Polymerization Lithography," *Carbon* 59 (2013): 283–288, https://doi.org/10.1016/j.carbon.2013.03.020.

63. M. Restaino, N. Eckman, A. T. Alsharhan, et al., "Situ Direct Laser Writing of 3D Graphene-Laden Microstructures," *Advanced Materials Technologies* 2100222 (2021): 2100222.

64. A. Ovsianikov, J. Viertl, B. Chichkov, et al., "Ultra-low Shrinkage Hybrid Photosensitive Material for Two-photon Polymerization Microfabrication," *ACS Nano* 2 (2008): 2257–2262, https://doi.org/10.1021/nn800451w.

65. M. Farsari and B. N. Chichkov, "Two-photon fabrication," *Nature Photonics* 3 (2009): 450–452, https://doi.org/10.1038/nphoton.2009.131.

66. L. Pertoldi, V. Zega, C. Comi, and R. Osellame, "Dynamic Mechanical Characterization of Two-photon-polymerized SZ2080 Photoresist," *Journal of Applied Physics* 128 (2020): 175102, https://doi.org/10.1063/5.0022367.

67. D. Jang, L. R. Meza, F. Greer, and J. R. Greer, "Fabrication and Deformation of Three-dimensional Hollow Ceramic Nanostructures," *Nature Materials* 12 (2013): 893–898, https://doi.org/10.1038/nmat3738.

68. L. R. Meza, S. Das, and J. R. Greer, "Strong, Lightweight, and Recoverable Three-dimensional Ceramic Nanolattices," *Science (1979)* 345 (2014): 1322.

69. A. Maggi, H. Li, and J. R. Greer, "Three-dimensional Nano-architected Scaffolds With Tunable Stiffness for Efficient Bone Tissue Growth," *Acta Biomaterialia* 63 (2017): 294–305, https://doi.org/10.1016/j.actbio.2017.09.007.

70. F. Kotz, A. S. Quick, P. Risch, et al., "Two-Photon Polymerization of Nanocomposites for the Fabrication of Transparent Fused Silica Glass Microstructures," *Advanced Materials* 33 (2021): 2006341, https://doi.org/10.1002/adma.202006341.

71. E. D. Lemma, F. Rizzi, T. Dattoma, et al., "Mechanical Properties Tunability of Three-Dimensional Polymeric Structures in Two-Photon Lithography," *Ieee Transactions on Nanotechnology* 16 (2017): 23.

72. S. O. Catt, C. Vazquez-Martel, and E. Blasco, "Investigating the Design of Macromolecular-based Inks for Two-photon 3D Laser Printing," *Molecular Systems Design & Engineering* 10 (2024): 176–183, https://doi.org/10.1039/d4me00160e.

73. D. Dzikonski, E. Bekker, R. Zamboni, et al., "Hybrid Microfluidic Chip Design With Two-Photon Polymerized Protein-Based Hydrogel Microstructures for Single Cell Experiments," *Advanced Materials Technologies* 10 (2025): 2401571, https://doi.org/10.1002/admt.202401571.

74. Q. Hu, G. A. Rance, G. F. Trindade, et al., "The Influence of Printing Parameters on Multi-material Two-photon Polymerisation Based Micro Additive Manufacturing," *Additive Manufacturing* 51 (2022): 102575, https://doi.org/10.1016/j.addma.2021.102575.

75. G. Minnick, T. Goldsmith, B. Tajvidi Safa, et al., "Toward Standardized Microscale Tensile Testing for Two-Photon Polymerization-Fabricated Materials in Liquid," *Small Science* 5 (2025): 2500228, https://doi.org/10.1002/smsc.202500228.

76. C. S. Shin, T. J. Li, and C. L. Lin, "Alleviating Distortion and Improving the Young's Modulus in Two-photon Polymerization Fabrications," *Micromachines (Basel)* 9 (2018): 615, https://doi.org/10.3390/mi9120615.

77. M. Gernhardt, E. Blasco, M. Hippler, et al., "Tailoring the Mechanical Properties of 3D Microstructures Using Visible Light Post-Manufacturing," *Advanced Materials* 31 (2019): 1901269, https://doi.org/10.1002/adma.201901269.

78. H. Leonards, S. Engelhardt, A. Hoffmann, et al., "Advantages and Drawbacks of Thiol-ene Based Resins for 3D-printing," *Proceedings of SPIE* 9353 (2015): 93530F.

79. Y. Jia, C. A. Spiegel, A. Welle, et al., "Covalent Adaptable Microstructures via Combining Two-Photon Laser Printing and Alkoxyamine Chemistry: Toward Living 3D Microstructures," *Advanced Functional Materials* 33 (2023): 2207826, https://doi.org/10.1002/adfm.202207826.

80. C. M. Kurpiers, S. Hengsbach, and R. Schwaiger, "Architectural Tunability of Mechanical Metamaterials in the Nanometer Range," *MRS Advances* 6 (2021): 507–512, https://doi.org/10.1557/s43580-021-00094-1.

81. A. Vyatskikh, S. Delalande, A. Kudo, X. Zhang, C. M. Portela, and J. R. Greer, "Additive Manufacturing of 3D Nano-architected Metals," *Nature Communications* 9 (2018): 593, https://doi.org/10.1038/s41467-018-03071-9.

82. G. Seniutinas, A. Weber, C. Padeste, I. Sakellari, M. Farsari, and C. David, "Beyond 100 Nm Resolution in 3D Laser Lithography — Post Processing Solutions," *Microelectronic Engineering* 191 (2018): 25–31, https://doi.org/10.1016/j.mee.2018.01.018.

83. L. Jonušauskas, D. Gailevičius, L. Mikoliunaite, et al., "Optically Clear and Resilient Free-form μ-optics 3D-printed via Ultrafast Laser Lithography," *Materials* 10 (2017): 12, https://doi.org/10.3390/ma10010012.

84. G. Konstantinou, E. Kakkava, L. Hagelüken, et al., "Additive Micromanufacturing of Crack-free PDCs by Two-photon Polymerization of a Single, Low-shrinkage Preceramic Resin," *Addit Manuf* 35 (2020): 101343.

85. P. Serles, M. Haché, J. Tam, et al., "Mechanically Robust Pyrolyzed Carbon Produced by Two Photon Polymerization," *Carbon* 201 (2023): 161–169, https://doi.org/10.1016/j.carbon.2022.09.016.

86. K. Baglo, M. Sauermoser, M. Lid, et al., "Overcoming the Transport Limitations of Photopolymer-Derived Architected Carbon," *Advanced Materials Technologies* 8 (2023): 2300092, https://doi.org/10.1002/admt.202300092.

87. X. Zhang, L. Zhong, A. Mateos, et al., "Theoretical Strength and Rubber-Like Behaviour in Micro-sized Pyrolytic Carbon," *Nature Nanotechnology* 14 (2019): 762–769, https://doi.org/10.1038/s41565-019-0486-y.

88. M. Bodaghi, L. Wang, F. Zhang, et al., "4D printing roadmap," *Smart Materials Structures* 33 (2024): 113501.

89. B. S. Calin and I. A. Paun, "A Review on Stimuli-Actuated 3D Micro/Nanostructures for Tissue Engineering and the Potential of Laser-Direct Writing via Two-Photon Polymerization for Structure Fabrication," *International Journal of Molecular Sciences* 23 (2022): 14270, https://doi.org/10.3390/ijms232214270.

90. C. A. Spiegel, M. Hippler, A. Münchinger, et al., "4D Printing at the Microscale," *Advanced Functional Materials* 30 (2019): 1907615, https://doi.org/10.1002/adfm.201907615.

91. B. Jian, H. Li, X. He, R. Wang, H. Y. Yang, and Q. Ge, "Two-photon Polymerization-based 4D Printing and Its Applications," *International Journal of Extreme Manufacturing* 6 (2024): 012001, https://doi.org/10.1088/2631-7990/acfc03.

92. M. Hippler, E. Blasco, J. Qu, et al., "Controlling the Shape of 3D Microstructures by Temperature and Light," *Nature Communications* 10 (2019): 232, https://doi.org/10.1038/s41467-018-08175-w.

93. J. Zheng, H. Yu, Y. Zhang, et al., "4D Printed Soft Microactuator for Particle Manipulation via Surrounding Medium Variation (Small 40/2024)," *Small* 20 (2024): 2311951, https://doi.org/10.1002/smll.202311951.

94. A. Ennis, D. Nicdao, S. Kolagatla, et al., "Two-Photon Polymerization of Sugar Responsive 4D Microstructures," *Advanced Functional Materials* 33 (2023): 2213947, https://doi.org/10.1002/adfm.202213947.

95. Y. Tao, L. Lin, X. Ren, et al., "Four-Dimensional Micro/Nanorobots via Laser Photochemical Synthesis towards the Molecular Scale," *Micromachines (Basel)* 14 (2023): 1656, https://doi.org/10.3390/mi14091656.

96. J. Y. Wang, F. Jin, X. Z. Dong, et al., "Dual-Stimuli Cooperative Responsive Hydrogel Microactuators via Two-Photon Lithography," *Small* 19 (2023): 2303166, https://doi.org/10.1002/smll.202303166.

97. L. V. Elliott, E. E. Salzman, and J. R. Greer, "Stimuli Responsive Shape Memory Microarchitectures," *Advanced Functional Materials* 31 (2021): 2008380, https://doi.org/10.1002/adfm.202008380.

98. G. Adam, A. Benouhiba, K. Rabenorosoa, C. Clévy, and D. J. Cappelleri, "4D Printing: Enabling Technology for Microrobotics Applications," *Advanced Intelligent Systems* 3 (2021): 2000216.

99. G. T. Iványi, B. Nemes, I. Gróf, et al., "Optically Actuated Soft Microrobot Family for Single-Cell Manipulation," *Advanced Materials* 36 (2024): 2401115, https://doi.org/10.1002/adma.202401115.

100. ISO, 527-2:2025 Plastics — Determination of tensile properties, 527-2:2025 Plastics — Determination of Tensile Properties, 2025.

101. ISO, 48-4:2018 Rubber, vulcanized or thermoplastic — Determination of hardness, 48-4:2018 Rubber, Vulcanized or Thermoplastic — Determination of Hardness, 2018.

102. T. Koch, W. Zhang, T. T. Tran, et al., "Approaching Standardization: Mechanical Material Testing of Macroscopic Two-Photon Polymerized Specimens," *Advanced Materials* 36 (2024): 2308497, https://doi.org/10.1002/adma.202308497.

103. E. S. Berkovich, "Three Faceted Diamond Pyramid for Micro Hardness Testing," *Industrial Diamond Review* 11 (1951): 129–132.

104. O. Eivgi, C. Vazquez-Martel, J. Lukeš, and E. Blasco, "Benchmarking Mechanical Properties of 3D Printed Elastomeric Microstructures," *Small Methods* 10 (2025): 2500432, https://doi.org/10.1002/smtd.202500432.

105. X. Gao, F. Hao, Z. Huang, and D. Fang, "Mechanics of Adhesive Contact at the Nanoscale: The Effect of Surface Stress," *International Journal of Solids and Structures* 51 (2014): 566–574, https://doi.org/10.1016/j.ijsolstr.2013.10.017.

106. S. Schweiger, T. Schulze, S. Schlipf, P. Reinig, and H. Schenk, "Characterization of two-photon-polymerization lithography structures via Raman spectroscopy and nanoindentation," *Journal of Optical Microsystems* 2 (2022): 033501, 10.1117/1.

107. B. C. Sousa, D. L. Cote, and J. Hay, "Toward an Instrumented Strength Microprobe—Origins of the Oliver-Pharr Method and Continued Advancements in Nanoindentation: Part 2," in *Elasticity of Materials*, ed. G. Akın Evingür and Ö. Pekcan (IntechOpen, 2023).

108. Z. Wang, W. M. Mook, C. Niederberger, R. Ghisleni, L. Philippe, and J. Michler, "Compression of Nanowires Using a Flat Indenter: Diametrical Elasticity Measurement," *Nano Letters* 12 (2012): 2289–2293, https://doi.org/10.1021/nl300103z.

109. J. Bauer, L. R. Meza, T. A. Schaedler, R. Schwaiger, X. Zheng, and L. Valdevit, "Nanolattices: An Emerging Class of Mechanical Metamaterials," *Advanced Materials* 29 (2017): 1701850, https://doi.org/10.1002/adma.201701850.

110. L. Valdevit and J. Bauer, "*Fabrication* of 3D Micro-/Nanoarchitected Materials," in *Three-Dimensional Microfabrication Using Two-Photon Polymerization*, ed. T. Baldacchini (Elsevier, 2020): 541–576.

111. Z. Vangelatos, K. Komvopoulos, and C. P. Grigoropoulos, "Regulating the Mechanical Behavior of Metamaterial Microlattices by Tactical Structure Modification," *Journal of the Mechanics and Physics of Solids* 144 (2020): 104112, https://doi.org/10.1016/j.jmps.2020.104112.

112. S. Czich, T. Wloka, H. Rothe, et al., "Two-Photon Polymerized Poly(2-Ethyl-2-Oxazoline) Hydrogel 3D Microstructures With Tunable Mechanical Properties for Tissue Engineering," *Molecules* 25 (2020): 5066, https://doi.org/10.3390/molecules25215066.

113. R. Cherukuri, A. Lambai, L. Sukki, et al., "In-situ SEM Micropillar Compression and Nanoindentation Testing of SU-8 Polymer up to 1000 s−1 Strain Rate," *Materials Letters* 358 (2024): 135824, https://doi.org/10.1016/j.matlet.2023.135824.

114. J. J. Roa, G. Oncins, J. Diaz, F. Sanz, and M. Segarra, "Calculation of Young's Modulus Value by Means of AFM," *Recent Patents on Nanotechnology* 5 (2011): 27.

115. L. Angeloni, M. Ganjian, M. Nouri-Goushki, et al., "Mechanical Characterization of Nanopillars by Atomic Force Microscopy," *Additive Manufacturing* 39 (2021): 101858, https://doi.org/10.1016/j.addma.2021.101858.

116. A. X. Cartagena-Rivera, W. H. Wang, R. L. Geahlen, and A. Raman, "Fast, Multi-frequency, and Quantitative Nanomechanical Mapping of Live Cells Using the Atomic Force Microscope," *Scientific Reports* 5 (2015): 11692, https://doi.org/10.1038/srep11692.

117. R. Coq Germanicus, D. Mercier, F. Agrebi, et al., "Quantitative Mapping of High Modulus Materials at the Nanoscale: Comparative Study Between Atomic Force Microscopy and Nanoindentation," *Journal De Microscopie* 280 (2020): 51.

118. H. Fischer, H. Stadler, and N. Erina, "Quantitative temperature-depending mapping of mechanical properties of bitumen at the nanoscale using the AFM operated With PeakForce Tapping TM mode," *Journal of Microscopy* 250 (2013): 210–217, https://doi.org/10.1111/jmi.12036.

119. S. Trusso, S. Firman, J. Balasubramanian, M. H. Khatami, H. de Haan, and N. R. Agarwal, "Correlating Topography and Viscoelastic Properties of Elastin-Like Polypeptide Scaffolds Probed at the Nanoscale: Intermodulation Atomic Force Microscopy," *Journal of the Mechanical Behavior of Biomedical Materials* 177 (2026): 107356, https://doi.org/10.1016/j.jmbbm.2026.107356.

120. H. Huang, I. Dobryden, P. A. Thorén, et al., "Local Surface Mechanical Properties of PDMS-silica Nanocomposite Probed With Intermodulation AFM," *Composites Science and Technology* 150 (2017): 111–119, https://doi.org/10.1016/j.compscitech.2017.07.013.

121. D. Platz, E. A. Tholén, D. Pesen, and D. B. Haviland, "Intermodulation Atomic Force Microscopy," *Applied Physics Letters* 92 (2008): 153106, https://doi.org/10.1063/1.2909569.

122. D. Silbernagl, P. Szymoniak, Z. Tavasolyzadeh, H. Sturm, and I. Topolniak, "Multiphoton Lithography of Interpenetrating Polymer Networks for Tailored Microstructure Thermal and Micromechanical Properties," *Small* 20 (2024): 2310580, https://doi.org/10.1002/smll.202310580.

123. M. Dudziak, I. Topolniak, D. Silbernagl, K. Altmann, and H. Sturm, "Long-time Behavior of Surface Properties of Microstructures Fabricated by Multiphoton Lithography," *Nanomaterials* 11 (2021): 3285, https://doi.org/10.3390/nano11123285.

124. J. F. Keckes, A. Jelinek, D. Kiener, and M. Alfreider, "Neural Network Supported Microscale In Situ Deformation Tracking: A Comparative Study of Testing Geometries," *JOM* 76 (2024): 2336.

125. J. Bauer, A. Guell Izard, Y. Zhang, T. Baldacchini, and L. Valdevit, "Programmable Mechanical Properties of Two-Photon Polymerized Materials: From Nanowires to Bulk," *Advanced Materials Technologies* 4 (2019): 1900146, https://doi.org/10.1002/admt.201900146.

126. W. P. Moestopo, S. Shaker, W. Deng, and J. R. Greer, "Knots Are Not for Naught: Design, Properties, and Topology of Hierarchical Intertwined Microarchitected Materials," *Science Advances* 10 (2023): eade6725, https://doi.org/10.1126/sciadv.ade6725.

127. A. R. Garcia-Taormina, T. Juarez, J. S. Oakdale, J. Biener, and A. M. Hodge, "Scaling-Up of Nano-Architected Microstructures: A Mechanical Assessment," *Advanced Engineering Materials* 21 (2019): 1900687, https://doi.org/10.1002/adem.201900687.

128. J. B. Forien, J. S. Oakdale, M. A. Worthington, and J. Biener, "Effect of Micron-scale Manufacturing Flaws on the Tensile Response of Centimeter Sized Two-photon Polymerization Microlattices," *MRS Commun* 11 (2021): 189–196, https://doi.org/10.1557/s43579-021-00033-z.

129. D. R. Cayll, I. S. Ladner, J. H. Cho, S. K. Saha, and M. A. Cullinan, "A MEMS Dynamic Mechanical Analyzer for in Situ Viscoelastic Characterization of 3D Printed Nanostructures," *Journal of Micromechanics and Microengineering* 30 (2020): 075008, https://doi.org/10.1088/1361-6439/ab8bc8.

130. A. Jelinek, S. Zak, M. J. Cordill, D. Kiener, and M. Alfreider, "Nanoscale Printed Tunable Specimen Geometry Enables High-throughput Miniaturized Fracture Testing," *Materials and Design* 234 (2023): 112329, https://doi.org/10.1016/j.matdes.2023.112329.

131. A. Jelinek, S. Zak, M. Alfreider, and D. Kiener, "High-Throughput Micromechanical Testing Enabled by Optimized Direct Laser Writing," *Advanced Engineering Materials* 25 (2023): 2200288, https://doi.org/10.1002/adem.202200288.

132. Y. Kai, S. Dhulipala, R. Sun, et al., "Dynamic Diagnosis of Metamaterials Through Laser-induced Vibrational Signatures," *Nature* 623 (2023): 514–521, https://doi.org/10.1038/s41586-023-06652-x.

133. C. N. LaFratta and T. Baldacchini, "Two-photon polymerization metrology: Characterization methods of mechanisms and microstructures," *Micromachines (Basel)* 8 (2017): 101, https://doi.org/10.3390/mi8040101.

134. F. Cantoni, D. Maher, E. Bosler, et al., "Round-robin Testing of Commercial Two-photon Polymerization 3D Printers," *Additive Manufacturing* 76 (2023): 103761, https://doi.org/10.1016/j.addma.2023.103761.

135. M. P. Jeske, M. J. Bonino, X. Huang, D. R. Harding, Y. Lu, and M. Anthamatten, "Two-Photon Printing of Base-Catalyzed Resins Involving Thiol-Michael Network Formation," *Advanced Materials Technologies* 9 (2024): 2400100, https://doi.org/10.1002/admt.202400100.

136. L. Yang, A. Münchinger, M. Kadic, et al., "On the Schwarzschild Effect in 3D Two-Photon Laser Lithography," *Advanced Optical Materials* 7 (2019): 1901040, https://doi.org/10.1002/adom.201901040.

137. E. H. Waller and G. von Freymann, "Spatio-temporal Proximity Characteristics in 3D μ-printing via Multi-photon Absorption," *Polymers (Basel)* 8 (2016): 297, https://doi.org/10.3390/polym8080297.

138. C. Arnoux, L. A. Pérez-Covarrubias, A. Khaldi, et al., "Understanding and Overcoming Proximity Effects in Multi-spot Two-photon Direct Laser Writing," *Additive Manufacturing* 49 (2022): 102491, https://doi.org/10.1016/j.addma.2021.102491.

139. J. S. Oakdale, R. F. Smith, J. B. Forien, et al., "Direct Laser Writing of Low-Density Interdigitated Foams for Plasma Drive Shaping," *Advanced Functional Materials* 27 (2017): 1702425, https://doi.org/10.1002/adfm.201702425.

140. J. B. Mueller, J. Fischer, F. Mayer, M. Kadic, and M. Wegener, "Polymerization Kinetics in Three-Dimensional Direct Laser Writing," *Advanced Materials* 26 (2014): 6566–6571, https://doi.org/10.1002/adma.201402366.

141. M. D. Uchic, D. M. Dimiduk, J. N. Florando, and W. D. Nix, "Sample Dimensions Influence Strength and Crystal Plasticity," *Science (1979)* 305 (2004): 986.

142. D. Kiener and A. Misra, "Nanomechanical Characterization," *MRS Bulletin* 49 (2024): 214–223, https://doi.org/10.1557/s43577-023-00643-z.

143. V. Hahn, P. Kiefer, T. Frenzel, et al., "Rapid Assembly of Small Materials Building Blocks (Voxels) Into Large Functional 3D Metamaterials," *Advanced Functional Materials* 30 (2020): 1907795, https://doi.org/10.1002/adfm.201907795.

144. P. Kiefer, V. Hahn, M. Nardi, et al., "Sensitive Photoresists for Rapid Multiphoton 3D Laser Micro- and Nanoprinting," *Advanced Optical Materials* 8 (2020): 2000895, https://doi.org/10.1002/adom.202000895.

145. S. Gu, C. Mao, A. Guell Izard, et al., "3D nanolithography With metalens arrays and spatially adaptive illumination," *Nature* 648 (2025): 591–599, https://doi.org/10.1038/s41586-025-09842-x.

146. F. Klein, T. Striebel, J. Fischer, et al., "Elastic Fully Three-dimensional Microstructure Scaffolds for Cell Force Measurements," *Advanced Materials* 22 (2010): 868–871, https://doi.org/10.1002/adma.200902515.

147. E. D. Lemma, B. Spagnolo, F. Rizzi, et al., "Microenvironmental Stiffness of 3D Polymeric Structures to Study Invasive Rates of Cancer Cells," *Advanced Healthcare Materials* 6 (2017): 1700888, https://doi.org/10.1002/adhm.201700888.

148. F. Colombo, M. Taale, F. Taheri, et al., "Two-Photon Laser Printing to Mechanically Stimulate Multicellular Systems in 3D," *Advanced Functional Materials* 34 (2024): 2303601, https://doi.org/10.1002/adfm.202303601.

149. I. Lodhi, D. Gajula, D. K. Brown, et al., "Piezoresistive Micropillar Sensors for Nano-Newton Cell Traction Force Sensing," *Journal of Microelectromechanical Systems* 33 (2024): 395–402, https://doi.org/10.1109/JMEMS.2024.3382974.

150. A. Ali, A. Mitra, and B. Aïssa, "Metamaterials and Metasurfaces: A Review From the Perspectives of Materials, Mechanisms and Advanced Metadevices," *Nanomaterials* 12 (2022): 1027, https://doi.org/10.3390/nano12061027.

151. J. Sun and J. Zhou, "Metamaterials: The Art in Materials Science," *Engineering* 44 (2025): 145.

152. E. Yarali, A. A. Zadpoor, U. Staufer, A. Accardo, and M. J. Mirzaali, "Auxeticity as a Mechanobiological Tool to Create Meta-Biomaterials," *ACS Applied Bio Materials* 6 (2023): 2562.

153. G. Flamourakis, I. Spanos, Z. Vangelatos, et al., "Laser-made 3D Auxetic Metamaterial Scaffolds for Tissue Engineering Applications," *Macromolecular Materials and Engineering* 305 (2020): 2000238, https://doi.org/10.1002/mame.202000238.

154. W. Zhang, P. Soman, K. Meggs, X. Qu, and S. Chen, "Tuning the Poisson's Ratio of Biomaterials for Investigating Cellular Response," *Advanced Functional Materials* 23 (2013): 3226–3232, https://doi.org/10.1002/adfm.201202666.

155. E. Yarali, M. Klimopoulou, K. David, et al., "Bone Cell Response to Additively Manufactured 3D Micro-architectures With Controlled Poisson's Ratio: Auxetic vs. *non-auxetic meta-biomaterials*," *Acta Biomater* 177 (2024): 228.

156. N. Munding, M. Fladung, Y. Chen, et al., "Bio-Metamaterials for Mechano-Regulation of Mesenchymal Stem Cells," *Advanced Functional Materials* 34 (2024): 2301133, https://doi.org/10.1002/adfm.202301133.

157. H. Yu, Q. Zhang, B. P. Cumming, et al., "Neuron-Inspired Steiner Tree Networks for 3D Low-Density Metastructures," *Advanced Science* 8 (2021): 2100141, https://doi.org/10.1002/advs.202100141.

158. K. Vanmol, A. A. Abdul Nazar, H. Thienpont, F. Ferranti, and J. Van Erps, "Fabrication of Multilevel Metalenses Using Multiphoton Lithography: From Design to Evaluation," *Optics Express* 32 (2024): 10190, https://doi.org/10.1364/OE.514237.

159. W. Choi, W. P. Moestopo, S. Gu, et al., "Helical Photonic Metamaterials for Encrypted Chiral Holograms," *Advanced Science* 12 (2025): 07931, https://doi.org/10.1002/advs.202507931.

160. M. A. Bessa, P. Glowacki, and M. Houlder, "Bayesian Machine Learning in Metamaterial Design: Fragile Becomes Supercompressible," *Advanced Materials* 31 (2019): 1904845, https://doi.org/10.1002/adma.201904845.

161. L. Cheng, T. Tang, H. Yang, et al., "The Twisting of Dome-Like Metamaterial From Brittle to Ductile," *Advanced Science* 8 (2021): 2002701, https://doi.org/10.1002/advs.202002701.

162. V. P. Stinson, U. Subash, M. K. Poutous, and T. Hofmann, "Towards Two-Photon Polymerization-Compatible Diffractive Optics for Micro-Mechanical Applications," *Micromachines (Basel)* 14 (2023): 1319, https://doi.org/10.3390/mi14071319.

163. P. Gaso, D. Jandura, S. Bulatov, D. Pudis, and M. Goraus, "Advancing Atomic Force Microscopy: Design of Innovative IP-Dip Polymer Cantilevers and Their Exemplary Fabrication via 3D Laser Microprinting," *Coatings* 14 (2024): 841, https://doi.org/10.3390/coatings14070841.

164. G. Mathew, E. D. Lemma, D. Fontana, et al., "Site-Selective Biofunctionalization of 3D Microstructures via Direct Ink Writing," *Small* 20 (2024): 2404429, https://doi.org/10.1002/smll.202404429.

165. G. Oguguo, A. Tanguy, S. Hallais, and L. Bodelot, "Characterization and Compensation of Distortions in Complex 3D Architected Microstructures Printed by Two-photon Polymerization," *Journal of Manufacturing Processes* 149 (2025): 229–240, https://doi.org/10.1016/j.jmapro.2025.05.039.